Ionic co-assembly in mixtures of polysaccharides and surfactants

vorgelegt von

Master of Science Leonardo Chiappisi

geboren in Palermo, Italien

von der Fakultät II - Mathematik und Naturwissenschaften

der Technischen Universität Berlin

zur Erlangung des akademischen Grades

Doktor der Naturwissenschaften

Dr.rer.nat.

genehmigte Dissertation

Promotionsausschuss:

Vorsitzender: Prof. Roderich Süssmuth (Technische Universität Berlin)

Gutachter: Prof. Michael Gradzielski (Technische Universität Berlin)

Gutachter: Dr. Giuseppe Lazzara (Università degli Studi di Palermo)

Tag der wissenschaftlichen Aussprache: 23. Februar 2015

Berlin 2015

The scientist does not study nature because it is useful to do so. He studies it because he takes pleasure in it, and he takes pleasure in it because it is beautiful.

Henri Poincaré

Acknowledgements

This is probably the most important section of this thesis, as the work in this form could have never seen light without the vivid environment of the Stranski Laboratorium at the Technische Universität Berlin. There is a large number of people which I want to acknowledge, as all of them have given their contribution making the last years spent at the TU-Berlin a great time.

First, I want to acknowledge my supervisor, Prof. Dr. Michael Gradzielski. I could find in him the right balance of supervision without being limited in my research. Thanks for quickly answering my emails (more than 300 in 2013 and 2014), and being in general very present. I enjoyed all, well most, of the also lengthy discussions, not only those directly concerning the current research. I learned with him, that you can spend incredible twenty minutes discussing about the temperature of the north sea in September.

A deep "THANKS!!!" goes to Sylvain Prévost. First, for his patience. With incredible regularity he was answering my questions, every day, several times per day over a period of years. To share the office with him definitely gave a boost to my understanding of scattering experiments and the way of extracting some useful information from weird-looking curves. I am also thankful to Ingo, Andreas, Caro, and the many more people who helped me in these years.

I would like also to thank Miriam and Ninh, who did a great job. It is a joy to see when the time spent on explanations is transformed into valuable results.

However, the Stranski-Lab is not only a great place to work at, but is a place where I could find a number of people whom it was a pleasure to spend also some free time with. Coffee breaks, cheese-evenings, bierchen or windsurfing are an important part of the last years. Thanks for that and I hope that all these activities will continue in the future.

A special thanks goes to Samantha, who every day recharges my batteries and gives the good mood needed for enjoying life. I thank you for all, even the shortest, moments spent together.

Finally, I would like to thank all those people who build up the foundation on which my whole life is based. Thanks for that to my family, which has continuously supported me, and to my school teachers. I am realizing only now how important those lessons were.

This cumulative thesis is based on following publications:

- **Paper I** Complexes of oppositely charged polyelectrolytes and surfactants – recent developments in the field of biologically derived polyelectrolytes. L. Chiappisi, I. Hoffmann and M. Gradzielski. *Soft Matter*, **2013**, *9*, 3896-3909.

- **Paper II** An improved method for analyzing isothermal titration calorimetry data from oppositely charged surfactant polyelectrolyte mixtures. L.Chiappisi, D. Li, N. J. Wagner, M. Gradzielski. *The Journal of Chemical Thermodynamics*, **2014**, *68*, 48-52. Supporting information available at dx.doi.org/10.1016/j.jct.2013.08.027

- **Paper III** Form factor of cylindrical superstructures composed of globular particles. L. Chiappisi, S. Prévost, M. Gradzielski. *Journal of Applied Crystallography*, **2014**, *47*, 827-834. Supporting information available at dx.doi.org/10.1107/S1600576714005524/fs5062sup1.pdf

- **Paper IV** Chitosan/Alkylethoxy Carboxylates: A Surprising Variety of Structures. L. Chiappisi, S. Prévost, I. Grillo, M. Gradzielski. *Langmuir*, **2014**, *30*, 1778-1787. Supporting information available at http://pubs.acs.org/doi/suppl/10.1021/la404718e

- **Paper V** From Crab Shells to Smart Systems: Chitosan–Alkylethoxy Carboxylate Complexes. L. Chiappisi, S. Prévost, I. Grillo, M. Gradzielski. *Langmuir*, **2014**, *30*, 10608-10616. Supporting information available at http://pubs.acs.org/doi/suppl/10.1021/la502569p

- **Paper VI** Towards bioderived intelligent nanocarriers for controlled pollutant recovery and pH-sensitive binding. L. Chiappisi, M. Simon, M. Gradzielski. *ACS applied Materials & Interfaces*, **2015**, *7*, 6139-6145. Supporting information available at http://pubs.acs.org/doi/suppl/10.1021/am508846r

- **Paper VII** Co-assembly in Chitosan – Surfactant mixtures: thermodynamics, structures and applications. L. Chiappisi, M. Gradzielski *Advances in Colloid and Interfaces*, **2015**, *220*, 92-107.

Herewith I ensure that the manuscripts were written by myself with the support of Prof. Dr. Michal Gradzielski, except for **Paper I**, where my contribution was focused on section 4. All experiments presented in the manuscripts were carried out by myself when not explicitly mentioned in the thesis. The data analysis was also performed by myself.

While performing the research with focus on polysaccharide / surfactant mixtures, I had the opportunity to come in contact with various quite different topics. Giving a contribution concerning scattering experiments (small-angle neutron scattering, static and dynamic light scattering), rheology measurements, and self-assembly of surfactants and polymers in general, the following additional papers were published in peer-reviewed journals.

1. Chiappisi, L.; Lazzara, G.; Milioto, S.; Gradzielski, M. A Quantitative Description of Temperature Induced Self-Aggregation Thermograms Determined by Differential Scanning Calorimetry. Langmuir 2012, 28, 17609–17616.

2. Kaur, G.; Chiappisi, L.; Prévost, S.; Schweins, R.; Gradzielski, M.; Mehta, S. K. Probing the Microstructure of Nonionic Microemulsions with Ethyl Oleate by Viscosity, ROESY, DLS, SANS, and Cyclic Voltammetry. Langmuir 2012, 28, 10640–10652.

3. Inal, S.; Chiappisi, L.; Kölsch, J. D.; Kraft, M.; Appavou, M.-S.; Scherf, U.; Wagner, M.; Hansen, M. R.; Gradzielski, M.; Laschewsky, A.; et al. Temperature-Regulated Fluorescence and Association of an Oligo(ethyleneglycol)methacrylate-Based Copolymer with a Conjugated Polyelectrolyte-The Effect of Solution Ionic Strength. J. Phys. Chem. B 2013, 117, 14576–14587.

4. Inal, S.; Kölsch, J. D.; Chiappisi, L.; Janietz, D.; Gradzielski, M.; Laschewsky, A.; Neher, D. Structure-Related Differences in the Temperature-Regulated Fluorescence Response of LCST Type Polymers. J. Mater. Chem. C 2013, 1, 6603.

5. Inal, S.; Kölsch, J. D.; Chiappisi, L.; Kraft, M.; Gutacker, A.; Janietz, D.; Scherf, U.; Gradzielski, M.; Laschewsky, A.; Neher, D. Temperature-Regulated Fluorescence Characteristics of Supramolecular Assemblies Formed By a Smart Polymer and a Conjugated Polyelectrolyte. Macromol. Chem. Phys. 2013, 214, 435–445.

6. Schwarze, M.; Chiappisi, L.; Prévost, S.; Gradzielski, M. Oleylethoxycarboxylate - An Efficient Surfactant for Copper Extraction and Surfactant Recycling via Micellar Enhanced Ultrafiltration. J. Colloid Interface Sci. 2014, 421, 184–190.

7. Wu, C.; Strehmel, C.; Achazi, K.; Chiappisi, L.; Dernedde, J.; Lensen, M. C.; Gradzielski, M.; Ansorge-Schumacher, M. B.; Haag, R. Enzymatically Cross-Linked Hyperbranched Polyglycerol Hydrogels as Scaffolds for Living Cells. Biomacromolecules 2014, 15, 3881-3890.

8. Schwarze, M.; Gross, M.; Buchner, G.; Kapitzki, L.; Chiappisi, L.; Gradzielski, M. Micellar Enhanced Ultrafiltration of Metal Cations with Oleylethoxycarboxylate. Journal of membrane science. **2015**, *478*, 140-147.

It should be mentioned here, that the results concerning the use of oleyl-ethoxycarboxylates for metal recovery (Papers 6 and 8) are based on the stimuli-responsive behaviour of alkyl oligoethyleneoxide carboxilic acids. Their investigation was a relevant part of the thesis and discussed in detail within the broader field of mixtures with oppositely charged chitosan (**Papers IV**, **V**, and **VI**) .

Contents

Abstract

In this thesis, the co-assembly of ionic polysaccharides and oppositely charged surfactants is investigated, with particular attention on chitosan – alkyl oligo-ethyleneoxide carboxylic acid mixtures.

The goal of the work is to evidence how the chemical structure of the polysaccharides influences the binding behaviour of oppositely charged surfactants and to determined how it affects the resulting structures. A main focus on modified cellulose and chitosan is given. An approach for extracting the most important thermodynamic binding parameters, e.g., free energy, enthalpy and entropy, from isothermal titration calorimetry is presented and successfully applied to mixtures of cationically modified cellulose and dodecyl sulfate. Moreover, a scattering form factor which is able to describe the scattering pattern typically found in mixtures of stiff ionic polysaccharide and globular macroions is derived.

In addition to the general behaviour of polysaccharide – surfactant mixtures, a comprehensive and detailed investigation of chitosan – alkyl oligoethyleneoxide carboxylic acid complexes is presented. Different aspects of these mixtures were explored with a main focus on their structural diversity and on the possibility of controlling them by pH and surfactant molecular architecture. A surprisingly high variety is obtained by changing the degree of ionization of the surfactant *via* pH, therefore directly affecting the strength of interaction with the oppositely charged polymer. The already large spectrum of accessible structures can be further widened by choosing amphiphiles with appropriate length of hydrophilic and hydrophobic blocks, therefore controlling the spontaneous curvature of the surfactant aggregate.

The large control over the possible structures and functionality can finally be exploited for the formulations of multifunctional systems which can find application in different fields. As demonstrative examples, their use of these mixtures as efficient and selective recovery system for organic and inorganic pollutants is demonstrated. Moreover, a simple, one-step layer-by-layer functionalization of solid surfaces is performed.

In summary, ionic polysaccharide – surfactant mixtures are highly complex systems, being a great challenge to understand, and having a large potential in different fields.

Zusammenfassung

Die vorliegende Dissertation beschäftigt sich mit der Selbstaggregation von entgegengesetzt geladenen Polysacchariden und Tensiden, mit einen Schwerpunkt auf Mischungen aus Chitosan und Alkyl-oligoethylenoxid Carboxylsäuren. Insbesondere wurde der Einfluss der chemischen Struktur der Polysaccharide, vor allem Chitosan und modifizierte Zellulose, auf das Bindungsverhalten von entgegengesetzt geladenen Tenside und auf die resultierenden Strukturen untersucht. Ein verbesserter Ansatz, um die wichtigsten thermodynamischen Parameter des Bindungsprozesses, z.B., freie Enthalpie, Entropie und Enthalpie, aus isothermer Titrationskalorimetrie zu bestimmen, wird vorgestellt. Der hergeleitete Formalismus wurde dann erfolgreich angewandt, um die Bindung von Dodecylsulfat an kationisch-modifizierte Zellulose zu beschreiben. Desweiteren, würde ein neuer Streuformfaktor hergeleitet, um typische Streukurven aus Mischungen von steifen geladenen Polysacchariden und kugelförmigen Makroionen zu beschreiben.

Nachdem das allgemeine Verhalten von Mischung aus Polysacchariden und Tensiden untersucht wurde, wird eine detaillierte und umfassende Untersuchung von Chitosan und Alkyl-oligoethylenoxid Carboxylsäuren präsentiert. Diese Mischungen wurden aus mehreren Blickwinkeln betrachtet, mit dem Hauptfokus auf deren strukturelle Vielfalt und die Möglichkeit, diese durch pH Änderungen oder über die molekular Struktur der Tenside zu kontrollieren und zu steuern. Die Mischungen von Chitosan und Alkyl-oligoethylenoxid Carboxylsäuren, die globulare Mizellen bilden, zeigen eine überraschend große strukturelle Vielfalt, die stark vom Ionisierungsgrad der Tenside abhängt. Diese Vielfalt an Strukturen kann noch erweitert werden, indem Tenside mit unterschiedlichen Packungsparametern verwendet werden. Um dies zu erreichen, können Tenside mit unterschiedlichen Längen der hydrophilen und hydrophoben Blöcke ausgewählt werden.

Die weitreichende strukturelle Kontrolle kann zur Formulierung von multifunktionellen Systemen genutzt werden. Als Beispiele werden deren Anwendung für eine selektive und effiziente Rückgewinnung organischer und anorganischer Schadstoffe gezeigt, sowie die einfache ein-Schritt-Multischichtfunktionalisierung von festen Oberflächen.

Somit wird gezeigt, dass Mischungen aus entgegengesetzt geladenen Polysacchariden und Tenside hoch komplexe Systeme sind, deren Verständnis zwar eine Herausforderung darstellt aber ein großes Potential in verschiedensten Anwendungsbereichen birgt.

Because we don't think about future generations,
they will never forget us.

Henrik Tikkanen

1

Introduction

All breakthrough in human life-quality was associated with the mastering of widespread techniques, e.g., the controlled use of fire, the discovery of agriculture or the development of automated machines. The technical progress, however, is strictly linked to the ability to process raw materials, being them stones, wood or metals. The effect on everyday life arising from these progresses were so strong, that the history of mankind is divided in ages named after the ability to process stone, bronze, or iron.

Similarly, given the enormous impact which polymers have on our everyday life, the term "age of plastic" was coined to describe the 20th century.[1] Despite polymers have been in use since thousands of years, it was just in 1920 that the existence of high molecular weight molecules was described.[2] For these discoveries Hermann Stuadinger was awarded with the Nobel Prize in chemistry in 1953.[3] Since then the understanding of polymer chemistry and physics has dramatically increased, as well as their spreading in modern civilization. Already in 1941, Yarsley and Couzens predicted how polymer-based objects will be ubiquitous in our everyday life:[1]

> "This plastic man will come into a world of colour and bright shining surfaces where childish hands find nothing to break, no sharp edges, or corners to cut or graze, no crevices to harbour dirt or germs. [...] As he grows he cleans his teeth and brushes his hair with plastic brushes, clothes himself with in plastic clothes, writes his first lesson with a plastic pen and does his lessons in a

book bound with plastic." (Yarsley & Couzens, 1941)

The predictions of Yarsley and Couzens became dramatically true and nowadays synthetic polymers are present in every single aspect of modern life. The reason can easily be found in the ease of processing synthetic polymers: objects with virtually every desired shape, with a broad range of mechanical properties, covering the whole spectrum of colours can be manufactured at low cost and in large quantities. Though, all these advantages do not come without side effects, which were elegantly summarized by Hopewell *et al.*:[4]

"Around 4 per cent of world oil and gas production, a non-renewable resource, is used as feedstock for plastics and a further 3–4% is expended to provide energy for their manufacture. A major portion of plastic produced each year is used to make disposable items of packaging or other short-lived products that are discarded within a year of manufacture. These two observations alone indicate that our current use of plastics is not sustainable. In addition, because of the durability of the polymers involved, substantial quantities of discarded end-of-life plastics are accumulating as debris in landfills and in natural habitats worldwide."

(Hopewell *et al.*, 2009)

Accordingly, within the perspective of a sustainable economy there is an increasing search for alternative polymers, which are obtained from renewable resources and/or are easily degradable. We can distinguish between biopolymers and bio-based polymers (often referred to as bioplastics). According to the IUPAC definition:[5]

Biopolymer: Macromolecule (including proteins, nucleic acids, and polysaccharides) formed by living organisms.

and

Bio-based polymer: [Polymer] derived from the biomass or issued from monomers derived from the biomass.

In both cases, advantages and disadvantages can be pointed out. Biopolymers, as they are directly formed by living organisms are found in a highly complex environment and their purification is an essentially complex task, limiting in several cases the large scale production. These polymers are inherently biodegradable, though long times might be required. Differently, bio-based polymers are synthetic polymers prepared from monomers with

biological origin, or chemical modifications of biopolymers. The term "bio-based" indicates only the renewable origin of the macromolecules and does not imply any biodegradability. For instance, the fermentation of glucose is a major source for bio-monomers, e.g., lactic, succinic or glutammic acid.[6] If on one hand the efficiency of the fermentation processes is increasing due to new genetically modified bacterial strains, the separation of the final products from the fermentation broth is still a major challenge.[7] Moreover, in my personal opinion, the use of food stock such as corn or sugar cane represent an essential ethical limitation for the use of bio-based polymers as environmentally friendly alternative for petrochemicals. An alternative is given by the fermentation of agricultural waste products. Although the yield is lower when compared to the use of corn, agricultural waste does not require extra land and water consumption.[8]

Over billions of years, nature has developed a large number of highly complex molecules with the aim of executing very different functions: low-molecular weight surfactants (mostly phospholipids) spatially delimit the living cell and its compartments; oligo- and poly-peptide chains act as catalysts, transporters or structural elements; the genetic information is safeguarded and trasmitted by nucleic acids. Carbohydrates, which are found in a large range of molecular weights, from monosaccharides (ca. 180 g mol^{-1}), disaccharides (ca. 340 g mol^{-1}), oligosaccharides (500 – 1500 g mol^{-1}) and polysaccharides (Mw up to several MDa), cover very different functions: starch and glycogen are the principal energy storages in animals and plats, cellulose and chitin are the main structural elements of plants and arthropods. Oligosaccharides, present in glycoproteins and glycolipids, serve as markers for cellular recognition.

These are just few examples of how nature employs carbohydrates. It is fascinating to note the width of functions which molecules with a rather similar chemical structure can cover. Accordingly, carbohydrates represent the largest fraction of biopolymers, with cellulose and chitin being the most abundant polysaccharides in nature (estimated annual production of cellulose by photosynthesis is of 10^{11} tons[9]).

Chitin (poly-β(1-4)–D–N-acetylglucosamine) and cellulose (poly-β(1-4)–D–glucose) are the main structural elements in plants and arthropods, i.e., insects, arachnids, and crustaceans. These polymers are chemically rather similar, the C2 hydroxyl group of cellulose is exchanged with an N-acetyl-amine moiety (see chemical formulas in Fig. 1.1) in chitin. It is interesting to note that, despite the strong and evident differences between a tree and a shrimp, nature has used the same recipe to provide them with a strong structural element. Although cellulose has been used since the beginning of human history, e.g., cotton and paper, its first description from a chemical perspec-
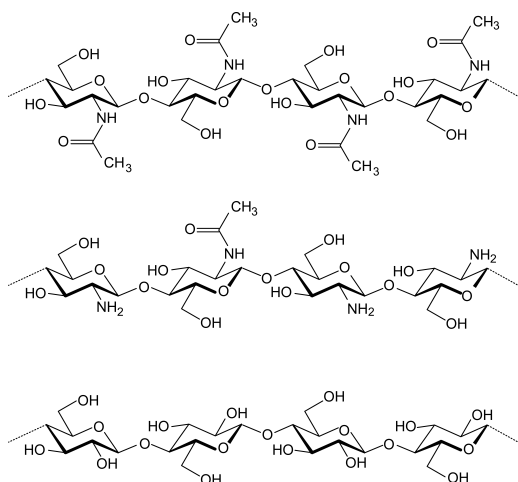
Figure 1.1 Chemical structure of, from top to bottom, chitin, chitosan and cellulose.

tive appeared only in 1838[10] (well before the concept of macromolecule was established). Chitin was first identified in 1929.[11]

Both cellulose and chitin are practically insoluble in water, despite their constituent units glucose and N-acetylglucosamine are highly soluble, 50 and 25 wt%, respectively. The low solubility of the macromolecules is the result of a complex interplay of forces, e.g., hydrophobic interactions, hydrogen bridging and van der Waals interactions.[12] Moreover, both polymers show a high tendency to crystallize and, in their natural environment, are found as a mixture of crystallites and amorphous regions.[13,14]

A clear advantage resulting from the numerous functional groups on the saccharidic backbone is the high variety in chemical modifications which can be performed on cellulose and chitin,[14–17] in particular, to overcome their insolubility in water. For instance, non-ionic cellulose esters, e.g., methyl- and hydroxypropyl cellulose, are soluble in cold water. At a first glance, it might seem contradicting that the substitution of an hydrophilic group $(-OH)$ with an hydrophobic one $(-OMe)$ increases the solubility of the polymer. This effect can be explained considering the increased free energy of the solid compound, in which favourable hydrogen bridges are broken and the crystallinity disrupted. The most common water-soluble derivative of chitin is chitosan (see chemical formula in figure 1.1). Chitosan is obtained from the partial or complete deacetylation of chitin, either *via* enzymatic or alkaline deacetylation.

Our everyday life is not only heavily influenced by non-ionic polymers, but also by polyelectrolytes, i.e., polymers with ionizable repeating units,
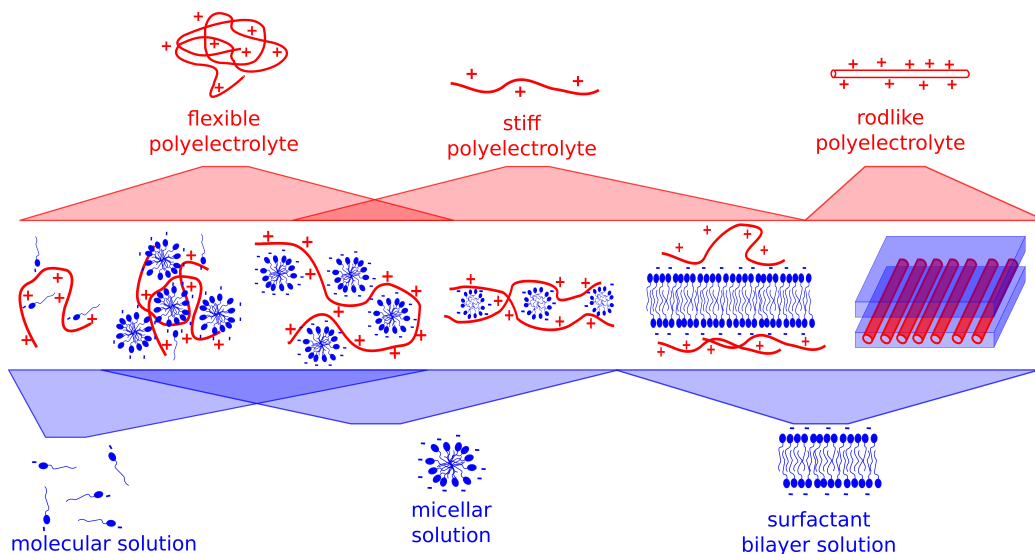
Figure 1.2 Schematic description of possible arrangements in surfactant – polyelectrolyte complexes depending on the polyelectrolyte stiffness and surfactant solubility and packing parameter. Adapted from *Soft Matter*, **2013**, *9*, 3896-3909.

are equally important. The behaviour of this class of polymers drastically differs from that of nonionic polymers in several aspects. The difference can be ascribed to the presence of N associated counterions for each polymer chain, with N being the number of charges on the polymer. The most obvious consequence of the presence of counterions is a dramatic increase of solubility of a polyelectrolyte in solvents with a high dielectric constant as compared to its nonionic counterpart. Moreover, electrostatic interactions are, in many cases, the dominant forces which control the properties of these systems.

In a number of cases, a synergistic use of polyelectrolytes and surfactants is desired, e.g., in paints or detergency, in which rheological control of the formulation, provided by the polyelectrolyte, has to be combined with the solubilization power and surface activity of surfactants. Accordingly, mixtures of polyelectrolytes and surfactants have been subject of studies since a long time.[18,19] The enormous range of properties which can be achieved in surfactant – polyelectrolyte complexes (SPECs) can be easily envisioned considering the virtually endless number of combinations of polymers and surfactants, the different conditions of concentration, ionic strength, pH, temperature, etc., in which these mixtures are prepared. A schematic representation of few possible structures is given in Fig. 1.2 (adapted from **Paper I**). It exceeds the goal of this thesis to discuss the large range of physico-chemical properties observed in such mixtures. However, there are some general points of polyelectrolyte – surfactant mixtures which are useful to be discussed to-

gether with the peculiarities of employing charged polysaccharides, as done in the next chapter.

*From time immemorial, man has desired to compre-
hend the complexity of nature in terms of as few
elementary concepts as possible.*

Abdus Salam

2

Overview on charged polysaccharide – surfactant mixtures

Related to: Soft Matter, **2013**, *9, 3896-3909.*

The behaviour of polyelectrolyte – surfactant mixtures strongly depends on a number of parameters. In addition to some intrinsic properties arising from the specific chemical nature of the polymer and of the surfactant, some general points of relevance are:

- **Mixing ratio** The mixing ratio, i.e., the relative amount of surfactant and polymer units, is probably the most important parameter governing the behaviour of such mixtures. The mixing ratio is in most cases defined as the ratio of nominal charges of surfactant and polyelectrolyte, i.e., $Z = [\text{Surf.}]/[\text{PE}]$, or *viceversa*. The use of nominal charges provides an alternative for the use of real charges, which are in many cases difficult to access.

  Around equimolarity, i.e., $Z = 1$, phase separation usually occurs, as the counterions, which provide to a large extent the solubility of the single compounds, are no longer associated with the macroions. The system can separate into two clear liquid phases (coacervation or associative phase separation) or into a solid precipitate in equilibrium with a clear solution (precipitation). In both cases, the complex rich phases

are mesoscopically ordered and can be used as a starting point for the preparation of highly structured and responsive solid materials.[20–23]

In the polyelectrolyte excess regime, i.e., for $Z < 1$, a particularly complex behaviour is observed, with a number of very different structures formed and properties observed, which depend on the chemical nature of the components and on the experimental conditions. In this region of the phase diagram, strong structural changes are observed when Z is approaching one, as a result of the mutual neutralization. Several cases are reported in which the viscosity of the system increases over orders of magnitude upon approaching the phase boundary as a consequence of an extended network formation with polyelectrolyte – surfactant micelles forming high energy knots.[24–27]

In the surfactant excess regime, i.e., for $Z > 1$, single polymer chains decorated by surfactant micelles are usually found. These solutions are, in most cases, clear and low-viscous. Despite being less interesting from a structural point of view, they deserve attention in a number of household products, which are mostly formulated in this region of the phase-diagram.[28]

- **Charge density of polyelectrolyte** The charge density of the polymer is a second parameter of major importance affecting the behaviour of mixtures with oppositely charged surfactants. In a primary instance, the charge density affects the polymer conformation, due to the electrostatic contribution to the persistence length (this point will be discussed in detail later in this chapter). Moreover, the binding constant found for a large number of SPECs varies with a ξ^2 power-law, ξ being the linear charge density of the polymer.[29] This empirical observation can be linked to the electrostatic repulsion U_e per unit length l which varies with the square of the charge density:

$$U_e \propto \frac{1}{l} \sum_i \frac{e_0^2}{r} = \frac{n_e e_0^2}{rl} = \xi^2 \qquad (2.1)$$

  with e_0, r, and n_e being the elementary charge, the spacing between them, and the number of charges per unit length, respectively. The charge density is then given by e_0/r or $n_e e_0/l$.

  Moreover, the polymer charge density also affects the conformational entropy contribution to the adsorption free energy. In particular, the conformation of free polymer in solution is that associated with the highest entropy; when the polymer is adsorbed onto the macroion (a soft or hard charged colloid), every contact point represents a constraint

reducing the overall polyelectrolyte conformational entropy. Large charge separation distances (when compared to the Kuhn length) are causing a minor entropic loss when compared to densely charged polyelectrolytes. It has to be pointed out here, that the entropic losses from the reduced conformational freedom of the polymer and from the association of several macroions into one complex are largely compensated by the release of counterions. Accordingly, in most cases the formation of surfactant – polyelectrolyte complexes is an entropically favoured process.

- **Molecular weight of polyelectrolyte** The molecular weight of the polyelectrolyte has a remarkable effect on the solubility, on the rheological properties, and to a certain extent on the structures found in polyelectrolytes – surfactant complexes. The higher the molecular weight of the polymer, the lower the entropy of mixing of the complex salt with the solvent, thereby simply decreasing the solubility of the SPECs.[30]
  As mentioned before, the addition of surfactant to a polyelectrolyte solution may lead to a substantial increase in viscosity as a result of the formation of an extended network. A necessary condition is, however, that the overlap concentration is reached. This last point is easily accomplished by employing polyelectrolytes on saccharidic basis, as they are mostly characterized by rather high molecular weights, e.g., which reaches several MDa.

- **Total concentration** The total concentration also affects the macroscopic behaviour of polyelectrolyte – surfactant mixtures. However, given the complexity of the system, it is everything but trivial to highlight some general effects. A first important aspect is that the addition (or removal) of solvent, alters the ionic strength and therefore the electrostatic interactions. Moreover, a dilution of the systems increases the translational entropy of the solutes. In certain cases this can lead to the counter-intuitive phenomenon of phase-separation upon dilution of polyelectrolyte – surfactant complexes.[31]

As mentioned before, the polymer conformation within the complex is one of the main structural directing forces, in addition to the spontaneous curvature of the surfactant aggregates. Moreover, similarly to a puzzle, the stability of the complexes largely depends on the spatial compatibility of the different "pieces", i.e., given by persistence lengths, curvatures, charge densities, *etc.*. With this in mind, remarkable differences between synthetic polyelectrolytes and ionic polysaccharides can be evidenced examining the effect of electrostatics on the polymer conformation. For most practical uses,

the electrostatic interaction in aqueous environment has to be considered. The spatial range of interaction is best described with two quantities: the Bjerrum length λ_B, i.e., the distance at which the energy of interaction of two point charges equals their thermal energy, and the Debye length δ, i.e., the distance at which the electrostatic potential has decayed of a factor of e.

$$\lambda_B = \frac{k_B T}{4\pi\varepsilon_0\varepsilon_r} \tag{2.2}$$

$$\delta = \sqrt{\frac{k_B T \varepsilon_0 \varepsilon_r}{2 N_A e_0^2 I}} \tag{2.3}$$

with k_B, T, ε_0, ε_r, and N_A being the Boltzmann constant, the temperature, the vacuum dielectric constant, the relative dielectric constant of the medium, and the Avogadro number, respectively. The ionic strength I is given by

$$I = \sum_i c_i z_i^2 \tag{2.4}$$

where c_i is the concentration of the ith species carrying a charge of $z_i e_0$. The Bjerrum and Debye lengths in water, at 300 K and at 0.15 mol L^{-1} ionic strength (physiological conditions) are $\lambda_B = 0.72$ and $\delta = 0.78$ nm, respectively. The fact that they are so close allows a fine tuning of electrostatic interactions in the sub-nm range, which seems to be a condition for the existence of higher forms of life.

The persistence length l_p of charged polymers can be expressed as the sum of the contributions of an intrinsic persistence length l_p^i and an electrostatic persistence length l_p^e:[32,33]

$$l_p \approx l_p^i + l_p^e \tag{2.5}$$

The former depends on the rigidity of the polymer backbone, the latter arises from the electrostatic repulsion between the charged units and accordingly, varies with the degree of ionization and/or ionic strength.

Most synthetic polyelectrolytes are based on vinyl monomers, e.g., polyacrylic acids, poly styrenesulfonate, with a rather flexible backbone (l_p of polyethylene is 0.65 nm[34]) and an average charge spacing of 0.25 nm. On the contrary, polysaccharides are characterized by a stiff backbone[35–37] ($l_p^i = 5 - 20$ nm) and a spacing between charges of 0.5 nm for the case of one charge on every glucosidic unit. Usually, the charge density is lower resulting in ca. 0.1 – 0.05 charges per nanometer. In summary, the conformation of synthetic polyelectrolytes is mostly determined by the electrostatic contribution to the persistence length while those of polysaccharides is rather given by their

intrinsic stiffness.

In co-assembled complexes with oppositely charged surfactants, the electrostatic contribution to the persistence length can be neglected in first approximation as most of the charges are compensated. Accordingly, one observes a strong reduction in persistence length for synthetic polyelectrolytes ($l_p \sim l_p^e$) while little variation takes place for ionic polysaccharides ($l_p \sim l_p^i$). The first consequence is that flexible (synthetic) polyelectrolytes show a higher affinity to curved surfaces when compared to ionic polysaccharides with a high intrinsic persistence length. Differently, ionic polysaccharides have a higher affinity towards flat surfaces, due to the minor conformation entropy loss upon adsorption. The effect of the high intrinsic persistence length of polysaccharides on the binding process and on the resulting structures in mixtures with oppositely charged surfactants will be discussed in detail in Chapters 3 and 4, respectively.

A theory is the more impressive the greater the simplicity of its premises, the more different kinds of things it relates, and the more extended its area of applicability.

Albert Einstein

3

Thermodynamics of polymer – surfactant mixtures

Related to: J. Chem. Therm., **2014**, *68, 48-52.*

The thermodynamic description of polyelectrolyte – surfactant mixtures is a fundamental part of a comprehensive understanding of their behaviour. In this chapter, an approach for extracting the most important thermodynamic parameters characterizing polyelectrolyte–surfactant mixtures from calorimetric experiments is provided. The function, which best connects the experimentally accessible information to thermodynamic quantities, such as Gibbs free energy, is the binding isotherm Θ. The binding isotherm is usually referred to as the "curve of the amount of ligands adsorbed as a function of the concentration or partial pressure of the ligand at a fixed temperature."[38] The first expression for an adsoprtion isotherm was given by Freundlich in 1909 and is purely based on empirical observations:[39]

$$\Theta = a\,p^{1/b} \tag{3.1}$$

where a and b are system specific parameters, and p the pressure/concentration of the adsorbing molecule. Irvin Langmuir first derived an expression for an adsorption isotherm based on the assumption that the adsorbed and

free gaseous molecules are in a dynamic equilibrium:[40,41]

$$\Theta = \frac{\mathrm{K}p}{1 + \mathrm{K}p} \tag{3.2}$$

with K being the equilibrium constant of the binding process. This expression is derived assuming no interaction between adsorbed molecules, i.e., K is independent from Θ. The binding constant immediately then leads to the standard Gibbs free energy of binding through

$$\Delta\mathrm{G}^\circ = -\mathrm{RT}\ln\mathrm{K} \tag{3.3}$$

The basic ideas derived in the early 20$^{\text{th}}$ century are valid also for complex polyelectrolyte/surfactant mixtures, although clear differences have to be considered. First, there is a strong interaction between the adsorbed surfactant molecules, primarily hydrophobic interactions. Secondly, the polymer "binding sites" cannot always be modelled as a two-dimensional lattice of identical binding sites. Moreover, a number of additional equilibria, e.g., micellization or micelle/polyelectrolyte binding may have to be considered.

In the simplest, but still realistic approach, the polymer is modelled as a one-dimensional array of binding sites and only nearest neighbor interactions between the surfactant molecules are considered. Such an approach leads to the commonly known Satake-Yang binding isotherm,[42] named after Satake and Yang which derived the expression reported in Eq. 3.4 in 1976. However, the same problem had been solved six years earlier by Gerhard Schwarz.[43] The model is based on the presence of three equilibria: the non-cooperative binding with equilibrium constant K, the cooperative binding with equilibrium constant Ku and the equilibrium between non-cooperatively and cooperatively bound surfactant, with u being the cooperativity parameter.

$$\Theta = \frac{1}{2}\left(1 + \frac{\mathrm{K}uC_f - 1}{\sqrt{(\mathrm{K}uC_f - 1)^2 + 4\mathrm{K}C_f}}\right) \tag{3.4}$$

C_f is the free surfactant concentration. A schematic representation of the three equilibria is given in Fig. 3.1.

The Satake-Yang model, with its assumptions of a linear array of binding sites and a 1:1 stoichiometry, is particularly suited for the description of polysaccharide – surfactant mixtures for the following reasons:

- The intrinsic persistence length is larger than the unit repeating distance, validating the assumption of linear array, at least on the length scale of neighbour interactions.
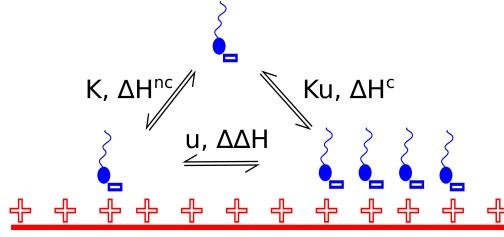
Figure 3.1 Schematic representation of the cooperative and non-cooperative binding as well as the transition between cooperatively and non-cooperatively bound surfactant molecules. Reprinted from *J. Chem. Therm.*, **2014**, *68*, 48-52, Copyright 2014, with permission from Elsevier.

- The 1:1 stoichiometry, i.e., one surfactant binds to one binding site, can be supported with simple geometrical considerations. The area per charge of a surfactant molecule and that of a saccharide unit are comparable. For instance, the headgroup area of sodium dodecyl sulfate is found to be between 60 and 55 Å^2, with a ionic strength between 25 and 200 mM, respectively.[44] In the crystalline form, i.e., when all charges are compensated, an effective headgroup area of 19.4 Å^2 is found.[45] Similar areas per charge are also found in ionic polysaccharides. Considering that a saccharide unit occupies an area of 5×5 Å^2, an area per charge of 25 and 75 Å^2 is found, provided every or every third unit is charged.

Within the Satake-Yang formalism, three states for the surfactant molecules are foreseen: free, non-cooperatively and cooperatively bound. Similarly, the polyelectrolyte binding site can be free, non-cooperatively and cooperatively occupied. The fraction of occupied binding sites which in Eq. 3.4; the fraction of bound sites which are non-cooperatively occupied is given by[43]

$$\chi = \frac{\text{K}C_f}{\lambda_0^2}\frac{1 - \Theta}{\Theta} \tag{3.5}$$

with λ_0 being

$$\lambda_0 = 0.5 \left(1 + \text{Ku}C_f + \sqrt{(\text{Ku}C_f - 1)^2 + 4\text{K}C_f} \right) \tag{3.6}$$

Any variation of an extensive property X of the system can be expressed as:

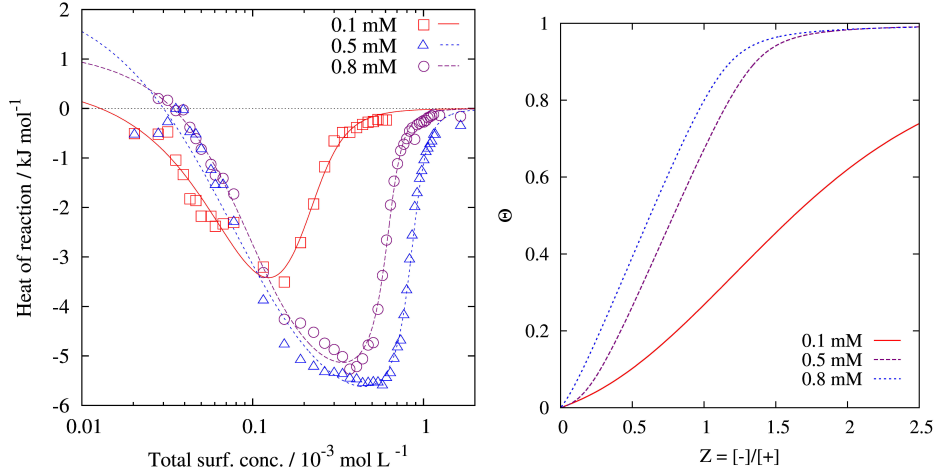$$\mathrm{d}X = \sum_i \overline{X}_i \mathrm{d}n_i \tag{3.7}$$

Figure 3.2 Binding heat (on the left) of sodium dodecyl sulfate to a cationiccally modified cellulose (JR-400) as a function of total surfactant concentration for different total binding site concentration. Lines are best fit curves obtained using Eq. 3.10. On the right, the resulting binding isotherms are reported.

where n_i and $\overline{X}_i$ are the moles and the partial molar quantity of the ith species. A comprehensive description of the system should take into account all six species present (in addition to the solvent), three states for the surfactant and three states for the polymer binding sites. However, Eq. 3.7 can be simplified, if the changes of the partial molar quantities of the solvent and the polymer binding sites are included in those of the surfactant:

$$\mathrm{d}X = \overline{X}_f \mathrm{d}n_f + \overline{X}_{nc} \mathrm{d}n_{nc} + \overline{X}_c \mathrm{d}n_c \tag{3.8}$$

with the pedices f, nc and c representing the free, non-cooperatively and cooperatively bound surfactant, respectively. With this premise, the heat exchanged during the binding process, which can be measured by isotherm titration experiments, is given by:

$$Q = \overline{H}_f \mathrm{d}n_f + \overline{H}_{nc} \mathrm{d}n_{nc} + \overline{H}_c \mathrm{d}n_c \simeq \Delta n_f \overline{H}_f + \Delta n_{nc} \overline{H}_{nc} + \Delta n_c \overline{H}_c \tag{3.9}$$

The same approach can be used for the description of other experimentally accessible quantities, e.g., the volume determined by densitometric experiments. In **Paper II**, from Eqs. 6 to 13 the derivation of an analytical expression for the description of ITC experimental data for systems following the Satake-Yang model is reported (see **Paper II** for symbols) that yields:

$$\overline{Q} = \frac{C_p \left(d\Theta/dC_f \right)}{C_p \left(d\Theta/dC_f \right) + 1} \left[\overline{\Delta \mathrm{H}} - \Theta \Delta \Delta \mathrm{H}^\circ \left(d\chi/d\Theta \right) \right] \tag{3.10}$$

15

Table 3.1 Thermodynamic binding parameters obtained for the adsorption of sodium dodecyl sulfate on a cationically modified cellulose (JR-400) for different polymer concentrations. The binding site concentration C_p is given in 10^{-3} mol L^{-1}, the standard binding free energies and enthalpies in 10^3 J mol^{-1} and the standard binding entropies in J K^{-1} mol^{-1}.

C_p	ΔG°_{nc}	ΔG°_c	$\Delta\Delta G\circ$	ΔH°_{nc}	ΔH°_c	$\Delta\Delta H^\circ$	ΔS°_{nc}	ΔS°_c	$\Delta\Delta S^\circ$
0.1	-29.3	-33.9	-4.6	5.0	-8.3	-13.3	111	83	-28
0.5	-26.9	-33.3	-6.4	8.8	-5.9	-14.7	116	89	-27
0.8	-27.5	-33.9	-6.4	5.9	-5.8	-11.7	108	91	-17

A python-written program to perform the fitting procedure is given in Appendix A.1. The application of the model derived to sodium dodecyl sulfate binding to a cationically modified cellulose (JR-400) is shown in Fig. 3.2. The model is able to describe all the features of the calorimetric signal. Accordingly, non-cooperative and cooperative binding heats and constants can be determined (see Table 3.1 and Table 1 of **Paper II**), shading light on the thermodynamic origin of the binding process. Moreover, the adsorption isotherms can be easily obtained from the binding constants using Eq. 3.10 (example curves reported in Fig. 3.2, right).

For a total polymer unit concentration of 0.8 mM, a non-cooperative and cooperative binding enthalpy of respectively 5.9 and -5.8 kJ mol^{-1} were found, leading to a $\Delta\Delta H^\circ = -11.7$ kJ mol^{-1}. This value is in good agreement with the micellization enthalpy found for sodium dodecyl sulfate in water at 35 °C,[46] corroborating the hypothesis of hydrophobic interactions among the surfactant tails as origin of the cooperativity. Moreover, both cooperative and non-cooperative adsorption process are entropically favoured, with $\Delta S^\circ_{nc} = 108$ J K^{-1} mol^{-1} and $\Delta S^\circ_c = 91$ J K^{-1} mol^{-1}. While the cooperative binding entropy is expected to be positive, due to the release of bound counterions and water, the positive ΔS°_{nc} indicates that the vertical surfactant – polyelectrolyte interactions are not solely of electrostatic origin. It has to be mentioned here, that the non-cooperative adsoprtion process takes place at low surfactant concentration, where the uncertainty in the titration experiments is highest and in which a correct account for dilutions heats is not trivial. In addition to accurate experimental values obtained at low surfactant concentrations, titrations performed at different temperatures which reveal also the variations in heat capacity, would help in the interpretation of the data.

On Mondays, Wednesdays, and Fridays we use the wave theory; on Tuesdays, Thursdays, and Saturdays we think in streams of flying energy quanta or corpuscles.

William Henry Bragg

4

Structures in stiff-polymer – macroion mixtures

Related to: J. App. Cryst., **2014**, *47, 827-834.*

As discussed in Chapter 2, ionic polysaccharides retain their stiffness also within the complex with oppositely charged surfactants. The most obvious consequence is that, provided the inverse curvature of the macroion is smaller than the intrinsic persistence length of the polysaccharides, an efficient wrapping does not take place. An favourable complexation can, however, be obtained when a stiff polymer and small globular particles co-assemble in superstructures with cylindrical symmetry.

Several examples of polysaccharide complexes with charged soft and hard macroions with one-dimensionally ordered suprastructrues can be found in literature.[47–51] In Fig. 4.1 a cryo-TEM image of suprastructures obtained in 10 nm silica nanoparticles / chitosan mixtures is shown.[50]

In addition to electron microscopy, the fine details of such structures can be evidenced by small-angle neutron and X-ray scattering, provided a suitable model is available. In particular, due to the low-contrast conditions of polysaccharides with respect to D_2O and H_2O (for SANS and SAXS), in many cases the contributions of the polymers to the scattering curves are weak and in a first instance negligible.[49,50] Accordingly, these structures can be described with a model of N-aligned spherical (or spheroidal) particles
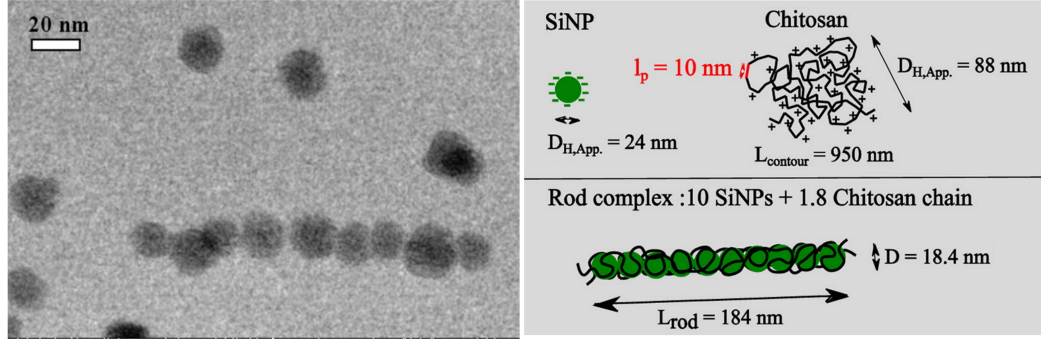
Figure 4.1 Cryo-TEM image of 0.01 g/L Chitosan and 10 g/L 10 nm silica nanoparticles, acetic acid buffer at 0.5 M total acetic acid and pH = 4.58 (top). Schematic representation of the structures found in solution, with characteristic lengths (bottom). Adapted with permission from *ACS Macro Lett.*, 2012, **1**, 857–861. Copyright 2014 American Chemical Society.

(Fig. 4.2, top). However, contrast variation experiments, in particular in neutron scattering, allow to focus also on the behaviour of the stiff polymer in the complex. For this case, a more complex model of N-aligned particles contained in a cylinder is needed (Fig. 4.2, bottom). Both models were derived in **Paper III** and applied to chitosan – alkyl oligoethyleneoxide carboxylic acid mixtures (**Paper IV** and **V**). Briefly, the scattering form factor of a cluster of N objects is given by:[53]

$$P(q, N) = \left\langle \left| \sum_{k=1}^{N} A_k(q) e^{-i\vec{q}\cdot\vec{r_k}} \right|^2 \right\rangle \tag{4.1}$$

where $A_k(q)$ is the scattering amplitude of the kth particle, located at a position $\vec{r_k}$; $\vec{q}$ is the scattering vector with modulus of:

$$q = \frac{2\pi \mathrm{n} \sin\left(\frac{\theta}{2}\right)}{\lambda} \tag{4.2}$$

with n being the refractive index (n = 1 for neutrons) and θ the scattering angle. The angle brackets represent the spatial average over all possible orientations. Eq. 4.1 can be solved applying the Euler relation for complex numbers and leads to the following solution for the case of N aligned identical particles, characterized by a scattering amplitude $A_{ob}(q)$:[52]

$$P(q, N) = \left\langle \frac{1 - \cos(z\,N)}{1 - \cos z} A_{ob}^2(q, \alpha) \right\rangle \tag{4.3}$$
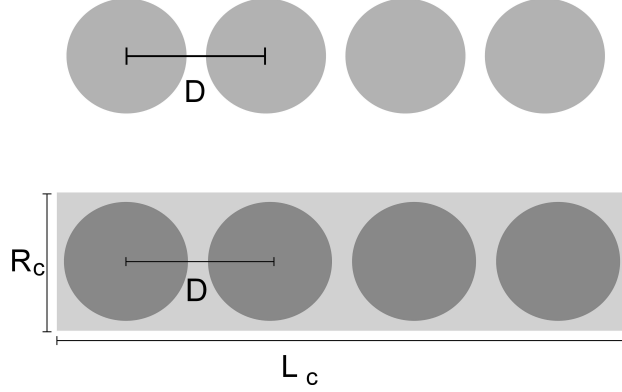
18

Figure 4.2 Schematic representation of the model on N aligned spheres, spaced by a distance D (top) and of N aligned spheres, spaced by a distance D, contained in a cylinder of radius R_c and length L_c (bottom). Adapted from Ref. 52 with permission of the International Union of Crystallography.

with $z = qD\cos\alpha$, where D is the modulus of the particle center-to-center distance vector $\vec{D}$ and α is the angle formed by $\vec{q}$ and $\vec{D}$.

For the case of N aligned identical particles, characterized by a scattering amplitude $A_{ob}(q)$, contained in a cylinder with scattering amplitude $A_{cyl}(q)$, the scattering intensity is:[52]

$$I_{tot}(q, N) = I_{Nob-Nob}(q, N) + I_{Cyl-Cyl}(q) + I_{Nob-Cyl}(q, N) \qquad (4.4)$$

where $I_{Nob-Nob}(q, N)$ is obtained as the product of Eq. 4.3 and $(\rho_{ob} - \rho_{cyl})^2$. $I_{Cyl-Cyl}(q)$ is given by:

$$I(q)_{Cyl-Cyl} = \left\langle (\rho_{cyl} - \bar{\rho})^2 A_{cyl}^2(q, \alpha) \right\rangle \qquad (4.5)$$

and

$$I_{Nob-Cyl}(q, N) = 2(\rho_{ob} - \rho_{cyl})(\rho_{cyl} - \bar{\rho}) \left\langle A_{ob}(q, \alpha) A_{cyl}(q, \alpha) g(N, z) \right\rangle \qquad (4.6)$$

with

$$g(N, z) = \left[\cos\left(\frac{z\,N}{2}\right) \sin\left(\frac{z\,N + z}{2}\right) - \sin\left(\frac{z}{2}\right) \right] \left[\sin\left(\frac{z}{2}\right) \right]^{-1} \qquad (4.7)$$

Features of the resulting curves are, from high to low-q, an increase in intensity, arising from the form factor of the spheroidal particle; the appearance of an asymmetric correlation peak at $q_p \simeq 2\pi/D$, whose intensity and sharpness increases with increasing number of particles, and a large q^{-1}-
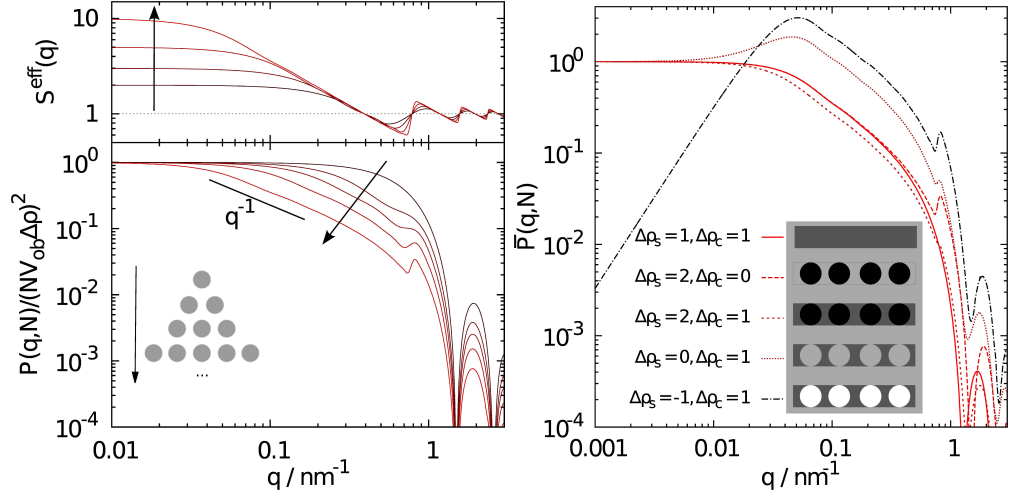
19

Figure 4.3 On the left, the normalized particle scattering form factor and effective structure factor, defined in Eq. 6 of **Paper III**, are reported as a function of the magnitude of the scattering vector, q, for objects with increasing number of spheres with radius of 3 nm with $N = 1, 2, 3, 5$ and 10 spaced by a center-to-center distance D of 8 nm. On the right, normalized particle scattering form factor from an object made up of ten spheres of radius 3 nm, with $D = 8$ nm included in a cylinder with radius of 3 nm and length $L = N \cdot D = 80$ nm, is reported for different contrast conditions as a function of q. Scattering contrasts are in arbitrary units. A schematic representation of the objects is given in the inset. Reproduced with permission of the International Union of Crystallography.

regime arising from the 1-dimensional symmetry of the object which persists till $q \simeq 2\pi/L_c$. Typical scattering curves are reported in Fig. 4.3 (and in Figures 2 and 7 of **Paper III**), which show the sensitivity of the obtained scattering curves to N and the contrast conditions. In particular the latter renders SANS experiments very interesting to characterize such structures. It is noteworthy, that the shape of the aligned objects is not limited to spheres, but every particle sharing a rotational axis with the cylinder can be used. For instance, the model was applied to the complexes formed by chitosan and alkyl oligoethyleneoxide carboxylic acids, self-assembling into core-shell ellipsoidal micelles.[48,49] A detailed description of these systems is given in next Chapter.

There is strength in numbers. When the bricks stick together, great things can be accomplished.

Steve Klusmeyer

5

Structural variety in chitosan/alkyl oligoethyleneoxide carboxylic acid complexes.

Related to: Langmuir, **2014**, 30, *1778-1787* & Langmuir, **2014**, 30, *10608-10616*.

In the previous chapters some peculiarities of polysaccharides were evidenced, in particular the effect on the binding process in mixtures with surfactants and on the resulting structures. Virtually all naturally occurring ionic polysaccharides are negatively charged, e.g., hyaluronate, carrageenans, alginate, *etc.*. Still, when working with mixtures of polyelectrolytes and oppositely charged surfactants, the use of polycations has several advantages, the most important being the lower toxicity of anionic surfactants, as compared to their cationic counterparts.

Nature does not provide cationic polysaccharides in large quantities. However, chitosan can be readily obtained from chitin, the second most abundant biopolymer after cellulose. Chitin is mostly extracted from crustaceans shells, i.e., a waste product of the food industry whose availability is estimated at ca. 60,000 - 80,000 tons per year.[54] Given the definitions in the first chapter, chitosan is not a biopolymer but rather a bioderived polymer, although

few fungi can synthesize chitosan directly.[55,56] It maintains the characteristics of biopolymers, e.g., renewable origin, high biodegradability and low toxicity for complex life forms. In addition, its pronounced antiinflammatory and antibacterial activities made this polymer particularly interesting for the medical industry.[57,58]

Accordingly, the interaction of chitosan with oppositely charged surfactants has attracted large interest in the past decades. Unfortunately, complexes of chitosan and strong anionic surfactants, e.g., sodium dodecyl sulfate, are characterized by a pronounced low solubility.[59–66] While this property can be exploited for the preparation of highly stable capsules,[59,63] it limits the field of uses of such mixtures.

A higher solubility of the complexes can be achieved by choosing a more hydrophilic surfactant. In addition, the use of a surfactant which shows a stimuli-responsive behaviour is a key requirement for the formulation of responsive supramolecular complexes. These considerations led to the choice of alkyl oligoethyleneoxide carboxylic acids. The used surfactants are, hereafter abbreviated as C_iE_jAc, with i and j being the number of carbon atoms and ethyleneoxide moieties, respectively; Ac represents one CH_2COOH unit. This class of surfactants shows a higher solubility as aliphatic acids, a pH-dependent behaviour given by the carboxylic headgoup, and a responsiveness towards temperature given by the oligoethyleneoxide moieties. A further advantage is given by the large choice of hydrophilic and hydrophobic block lengths, which allows to largely vary the packing parameter and the solubility of the surfactant.

In this work, surfactants with different alkyl chain length (C_8, C_{12}, and $C_{18:1}$), and varying number of ethyleneoxide units (2.5 – 10) were employed at different pH conditions (3.5 – 5.0). This pH-range was chosen as the degree of ionization of the surfactant is largely changed while that of chitosan remains almost constant (see Fig. 5.1). A summary of physico-chemical properties of the surfactants, i.e., critical micelle concentration, headgroup area requirement, packing parameter, etc., is given in Table 2 of **Paper V**.

The small-angle neutron scattering patterns arising from mixtures of chitosan with $C_{12}E_{10}Ac$, C_8E_5Ac, and $C_{12}E_{4.5}Ac$ at pH = 4, and with $C_{18:1}E_9Ac$ at different pH are reported in Fig. 5.2 (or Fig. 7 of **Paper IV** and Fig. 3 of **Paper V**). In all cases, strong structural changes are observed either when the degree of ionization of the surfactant is changed or by changing its molecular structure. In particular, $C_{18:1}E_9Ac$ and $C_{12}E_{10}Ac$, and C_8E_5Ac form globular micelles at the given experimental conditions; $C_{12}E_{4.5}Ac$ is found as a mixture of cylindrical and vesicular aggregates.[67] All experiments were carried out in a 0.2 M acetic acid buffer, in excess of chitosan. The mixing ratio, Z, is defined as the ratio of surfactant molecules over the glucosamine
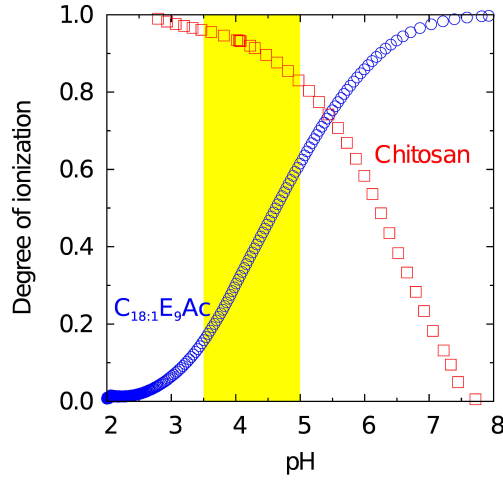
Figure 5.1 On the left, degree of ionization of a 1 wt% $C_{18:1}E_9Ac$ (open circles) and of a 1 wt% chitosan solution (open squares) in H_2O as a function of pH obtained from potentiometric titration. The box indicates the investigated pH range.

units of chitosan.

Effect of surfactant molecular architecture The choice of $C_{12}E_{10}Ac$, C_8E_5Ac, and $C_{12}E_{4.5}Ac$ allows a systematic investigation of the effect of the surfactant on the resulting structures. First, the surfactant solubility is varied keeping the packing parameter constant, $C_{12}E_{10}Ac$ *vs.* C_8E_5Ac, and, secondly, the surfactant curvature is changed keeping the solubility constant $C_{12}E_{10}Ac$ *vs.* $C_{12}E_{4.5}Ac$ (see parameters reported in Table 2 of **Paper V**). Small-angle neutron and light scattering experiments reveal a similar behaviour for all globular micelles at pH = 4.0: at low surfactant concentration the polymer chains are loosely decorated by surfactant micelles; at intermediate surfactant concentration the formation of linearly ordered aggregates is observed and their scattering pattern can be described with the models derived in Chapter 4; a further addition of surfactant causes the 1D structures to collapse into a core-shell suprastructure with a core formed by densely packed micelles surrounded by a stabilizing chitosan chain.

Highly different scattering patterns are obtained when chitosan and a vesicle-forming surfactant ($C_{12}E_{4.5}Ac$) are mixed. The curves are characterized by a large q^{-2}-law (typical for systems with a 2-dimensional extension, e.g., bilayers), the presence of a correlation peak at $q_p = 0.095 \text{nm}^{-1}$, and a sudden change in slope at $q \sim 0.09 \text{nm}^{-1}$. The curves can be described with a model of multiwalled vesicles in the presence of cylindrical surfactant aggregates (see details in **Paper V**). The one-step formation of such
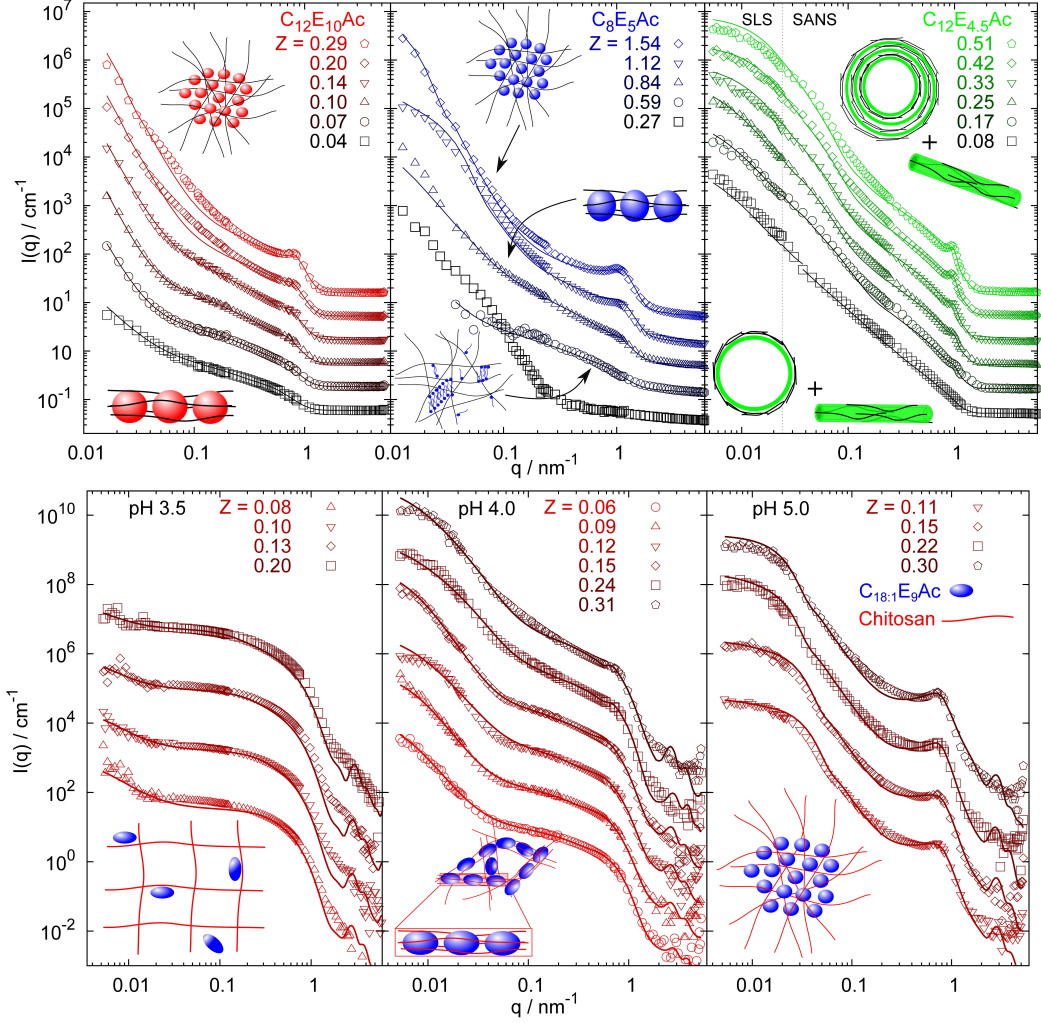
Figure 5.2 Top: SANS intensities for mixtures of $C_{12}E_{10}Ac$, C_8E_5Ac and $C_{12}E_{4.5}Ac$ and chitosan at 0.3 wt% chitosan at different $Z = [-]/[+]$ and pH $= 4$. Straight lines represent best fits according to different models (see **Paper V**). Curves are scaled by successive factors of 3. Reprinted with permission from *Langmuir*, **2014**, *30*, 10608-10616. Copyright 2014 American Chemical Society. Bottom: SANS intensity as a function of magnitude q of the scattering vector for mixtures of $C_{18:1}E_9Ac$ and chitosan at 0.3 wt% chitosan at different pH and chitosan to surfactant ratio $Z = [-]/[+]$. Straight lines represent best fits according to different models (see **Paper IV**). Curves are scaled by successive factors of 30, 10 and 20 for curves at pH 3.5, 4.0 and 5.0, respectively. Reprinted with permission from *Langmuir*, **2014**, *30*, 1778-1787. Copyright 2014 American Chemical Society.
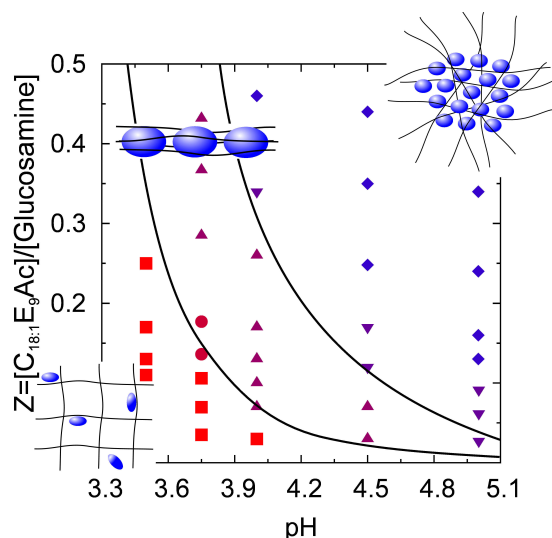
Figure 5.3 Structural phase diagram of mixtures of chitosan – $C_{18:1}E_9Ac$ micelles as a function of pH and mixing ratio and constant chitosan concentration of 0.3 wt% (in a 0.2 mol kg^{-1} acetate buffer). Full lines represent the ranges of the different structural arrangements. Adapted with permission from *Langmuir*, **2014**, *30*, 1778-1787. Copyright 2014 American Chemical Society.

multiwalled vesicles can be exploited for a polymer-surfactant layer-by-layer surface modification, as shown in Chapter 6. The corresponding scattering patterns are reported in the upper part of Fig. 5.2 and in **Paper V**.

In summary, the spontaneous shape of the surfactant aggregate is retained within the complex, and chitosan provides a framework for the supramolecular aggregation. Moreover, the surfactant spontaneous structure is also found when the complexes are separated out of solution, which were analysed by small-angle X-ray scattering (see Fig. 5 of **Paper V**). This provides an easy route for the formulation of solid materials, with an high mesoscopic order controlled by the molecular structure of the surfactant.

Effect of pH   Varying the pH of the solution between pH 3.5 and 5.0 directly affects the degree of ionization of the surfactant with little changes in that of the chitosan (see Fig. 5.1). Moreover, for the case of $C_{18:1}E_9Ac$ the micellar structure shows only minimal changes upon pH increase within the investigated pH-range.[68] These premises allow for the investigation of the effect of the strength of the surfactant/polymer interaction on the resulting structures with minimal side effect interferences. From the scattering curves shown in Fig. 5.2 (bottom), and the light scattering results reported in **Paper**
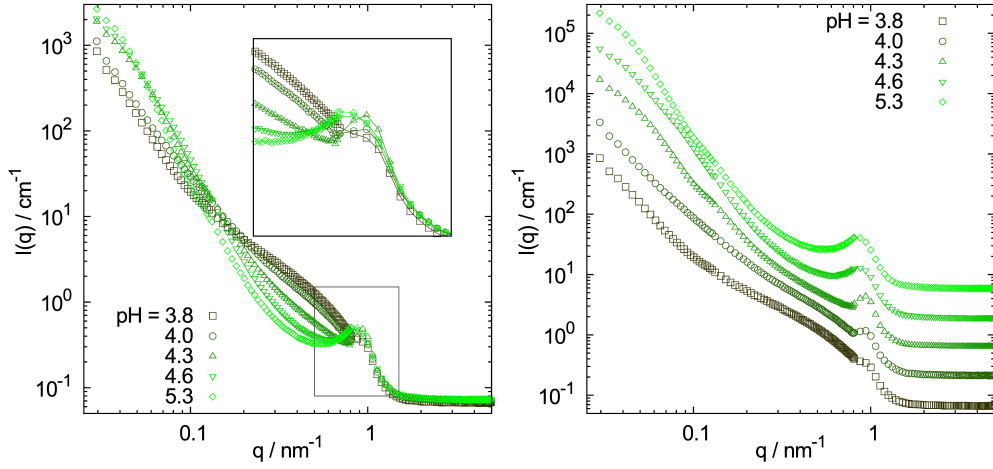
Figure 5.4 SANS intensity as a function of magnitude q of the scattering vector for mixtures of $C_{12}E_{4.5}Ac$ and chitosan at 0.3 wt% chitosan at different pH and chitosan to surfactant ratio $Z = [-]/[+] = 0.5$. On the right the curves are scaled by successive factors of 3. Experiments were performed on D11 at the Institut Laue-Langevin with a wavelength of $\lambda = 6$ Å, sample-to-detector distances of 1.2, 8 and 20 m with respective collimation of 5.5, 8.0 and 20.5 m.

IV, a comprehensive structural phase diagram can be constructed (see Fig. 5.3). As explained in detail in **Paper IV**, this structural evolution is a direct consequence of the delicate balance of forces, which are either pH-dependent (the binding of surfactant micelles and polymer chain) or pH-independent, such as the bending of the stiff chitosan. The transition between the different structures can be employed for the formulation of highly responsive delivery/recovery systems as shown in the next Chapter.

Even stronger structural changes are observed by pH-changes in chitosan – $C_{12}E_{4.5}Ac$ mixtures,with $Z = [-]/[+] = 0.5$ as reported in Fig. 5.4 (Unpublished data). With increasing pH, one observes:

- An increase in scattering intensity at low-q, with a jump between pH 4.0 and 4.3.

- The scattering curves measured at higher pH are approaching a plateau at low-q.

- An evident increase of the correlation peak at $q \approx 0.9$ nm^{-1}. The peak becomes also broader and shifts to smaller q values with increasing pH.

- A decrease in scattering intensity at intermediate scattering vectors ($0.02 < q/\text{nm}^{-1} < 0.06$), as commonly found for objects with increas-

26

ing compactness (and therefore showing minor fluctuations in the scattering length density at a length scale of $2\pi/q$).

To interpret these results it has to be recalled that $C_{12}E_{4.5}Ac$ aggregates themselves undergo strong structural changes with increasing pH.[67] At low pH a mixture of cylinders and large vesicles is found. The vesicles decrease in size with increasing pH. Above pH 4.5 a transition towards globular micelles is found. As shown before, multiwalled vesicles are formed at $Z = 0.5$ and pH $= 4$. With this premises, the scattering curves presented in Fig. 5.4 can be interpreted as follows:

- At pH $= 3.8$, chitosan and $C_{12}E_{4.5}Ac$ weakly interact. A mixture of cylindrical aggregates and vesicles with low bilayer multiplicity is probably formed, as indicated by the relatively high scattering at intermediate q, and the presence of a little pronounced correlation peak at $q \sim 0.9$ nm^{-1}.

- Upon increase of the pH, the interactions become stronger, the correlation peak becomes more pronounced, the scattering intensity at intermediate q decreases while that at low-q increases. Moreover, at pH 4.3, objects with a rather well defined size are formed, as indicated by the oscillations at $q \sim 0.1$ nm^{-1}. Presumably, multiwalled vesicles, with increased bilayer multiplicity and decreasing size are formed between pH 4.0 and 4.3.

- The curves recorded at higher pH (4.6 and 5.3) show a pronounced broadening of the correlation peak and a shift towards smaller q, which could arise from a transition from a 2-dimensional order (stacked lamellae) to a 3-dimensional one (densely packed micelles). The transition of the surfactant aggregates from a bilayer structure towards globular aggregates upon increasing degree of ionization was shown by other authors to occur at pH 4.5.[67]

Effect of ionic strength It was shown in several studies that the total ionic strength strongly affects the ionic co-assembly of polymers and surfactants.[66,69,70] The general effect is a weakening of the surfactant – polymer interactions,[66,69] due to a screened electrostatic interaction and to a reduced entropic gain from counterion release. Accordingly, several examples show that upon reaching rather high ionic strengths (ca. 1 M) the complexes can be dissolved into their components.[70] Moreover, an increasing ionic strength may also alter the structural behaviour of the complexes,[70] either as a consequence of dehydration of the supraaggregates or because it alters the curvature of the surfactant aggregate.
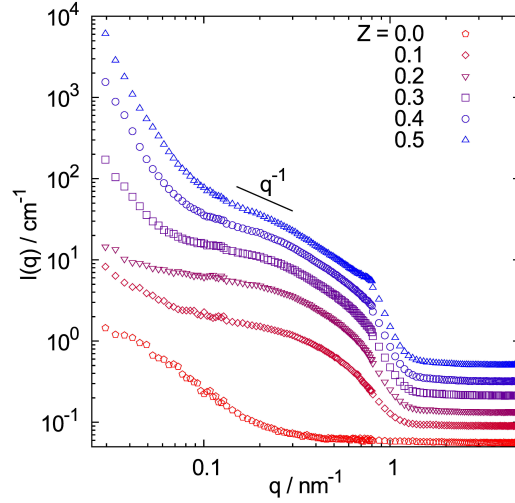
Figure 5.5 SANS intensity as a function of magnitude q of the scattering vector for mixtures of $C_{18:1}E_9Ac$ and chitosan at 0.3 wt% chitosan at pH = 4, increasing chitosan to surfactant ratio Z. Acetic acid concentration was 0 mM. Curves are scaled by successive factors of 1.5. Experiments were performed on D11 at the Institut Laue-Langevin with a wavelength of $\lambda = 6$ Å, sample-to-detector distances of 1.2, 8 and 20 m with respective collimation of 5.5, 8.0 and 20.5 m.

The effect of the total ionic strength on the co-assembly of chitosan and $C_{18:1}E_9Ac$ was investigated by preparing mixtures at different buffer concentration or by the addition of sodium chloride. Apparently contradicting results are found in these mixtures. In Fig. 5.5 the scattering patterns of chitosan – $C_{18:1}E_9Ac$, with a total concentration of acetic acid of 0 mM and at pH = 4.0 adjusted with a minimal amount of HCl are shown. The dependence of the molecular weight from the mixing ratio for complexes prepared at different buffer concentration is shown in Fig. 5.6. These results indicate that the addition of salt simply shifts the co-assembly process towards lower mixing ratios, without affecting the observed structures.

Further insight is obtained when the dependence of the molecular weight of the complex is reported as a function of the added salt concentration (see Fig. 5.6 right). A similar behaviour, showing a maximum binding affinity is reported for other polyelectrolyte – protein[71,72] or polyelectrolyte – surfactant complexes.[73–75] The non-monotonic trend indicates that more than one effect influences the co-assembly process.

As mentioned before, at high ionic strength the interaction between surfactant micelles and polyelectrolyte is strongly reduced as a consequence of the decreasing electrostatic interactions and entropy gain of freeing the coun-
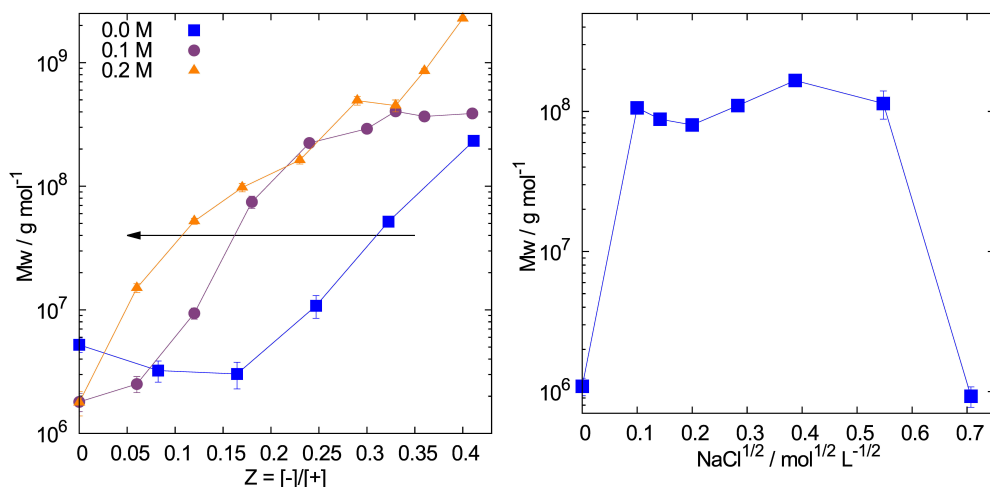
Figure 5.6 On the left, the molecular weight as determined from light scattering curves (for details refer to the experimental section of **Paper IV**) for mixtures of $C_{18:1}E_9Ac$ and chitosan at 0.3 wt% chitosan at pH $= 4$ at different chitosan to surfactant ratio Z and acetic acid concentration. pH was adjusted by addition of HCl. On the right, the molecular weight determined for mixtures of $C_{18:1}E_9Ac$ and chitosan at 0.3 wt% chitosan, pH $= 4.5$, $Z = [-]/[+] = 0.2$, acetic acid concentration of 0 mM and variable sodium chloride concentration is reported. Experiments were performed by Ninh Tran Dang during his "Forschungspraktikum" supervised by the author.

terions. Differently, an explanation for the salt-induced co-assembly is not trivial and the arguments reported in literature are system-specific[72,73,75] and cannot be applied to these mixtures. An initial hypothesis is that the vertical micelle – polymer interaction steadily decreases with increasing salt concentration; however, for the formation of large, dense supramolecular aggregates a collapse of the decorated polymer chains is needed. This collapse might be hindered by the micelle– micelle or polymer–polymer electrostatic repulsions and can take place only above a certain ionic strength. This example demonstrates the complexity of this systems, with a multitude of relevant forces influencing the co-assembly process.

As shown in the next chapter, these systems can be exploited for different purposes by employing surfactants with the most suitable packing parameters and controlling the co-assembly process *via* pH.

*A complex system that works is invariably found to
have evolved from a simple system that worked.*

John Gall

6

Uses of Chitosan/Alkyl oligoethyleneoxide carboxylic acid complexes

Related to: ACS Appl. Mater. Interfaces, **2015**, *7,
6139–6145.*

The high structural variety found in mixtures of chitosan and oppositely charged alkyl oligoethyleneoxide carboxylic acid forming globular micelles is summarized in the phase diagram reported in Fig. 5.3 and in **Paper IV**. The variation of the block length of the surfactants (at a given a packing parameter $p \sim 0.3$) does shift the structural phase boundaries but not their overall behaviour.

By varying the pH from 3.5 to 5.5, keeping the total acetic acid/acetate concentration of 0.2 mol kg^{-1}, chitosan concentration of 0.3 wt%, and $Z = [-]/[+] = 0.2$ constant, all structures formed in mixtures with $C_{18:1}E_9Ac$ are probed. In particular, the mobility of the surfactant micelles is expected to strongly decrease with increasing pH, as they become incorporated into the supramolecular complex. Their mobility on a time and space scale of ms and μm can be probed by fluorescence correlation spectroscopy (FCS), provided a fluorescent dye is permanently solubilized within the micellar core.
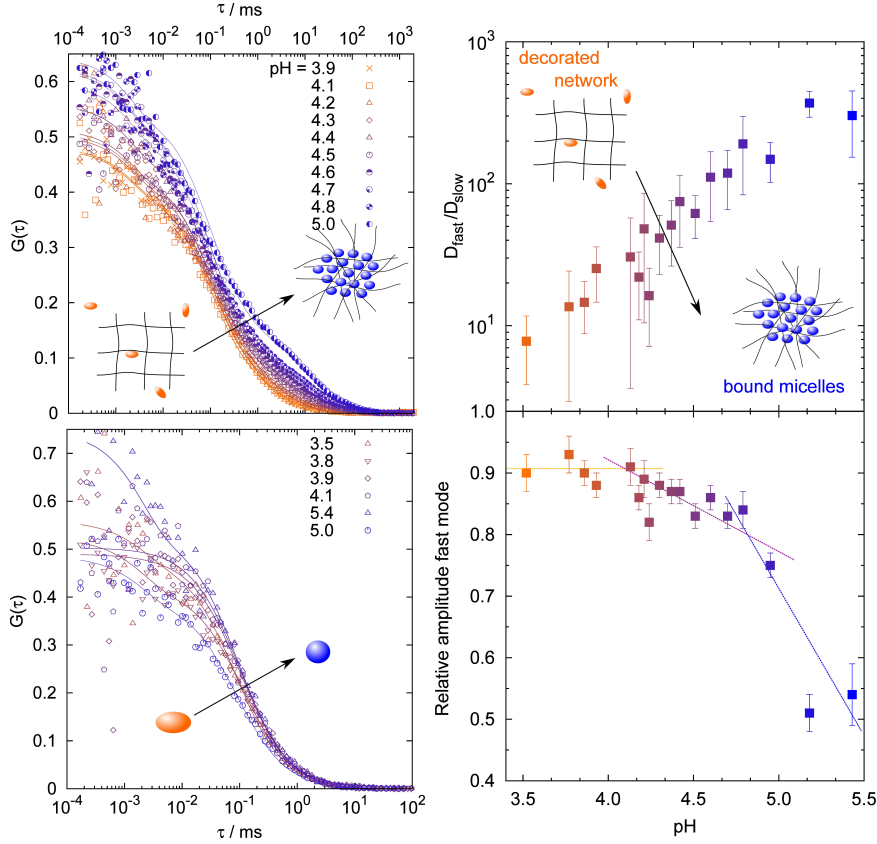
Figure 6.1 On the left: fluorescence autocorrelation functions with 5 nM Nile red recorded for chitosan - $C_{18:1}E_9Ac$ mixtures, with $Z = [-]/[+] = 0.2$, constant chitosan concentration of ~ 0.3 wt% and variable pH (top) and for $C_{18:1}E_9Ac$ 1 wt% solutions at variable pH (bottom). On the right: ratio of fast and slow diffusion coefficients (top) and relative amplitude of the fast mode as a function of pH (bottom). FCS experiments were performed by Miriam Simon in collaboration.

This was achieved by using Nile Red, whose binding constant to $C_{18:1}E_9Ac$ is estimated to be 1.5 ± 0.2 μM^{-1}. The obtained correlation functions are reported in Fig. 6.1 and in **Paper VI**. The incorporation of the surfactant micelles in the complex can be clearly seen in the appearance of a second, slow mode for pH > 4. Moreover, the transition between the different structural phase regions can be seen in the change of slope of the relative amplitudes of the slow and the fast mode on pH (see Fig. 6.1).

This pH-dependent binding/release of the surfactant micelles can be exploited for the formulation of release and recovery systems. In particular, the use of chitosan $- C_{18:1}E_9Ac$ complexes for the recovery of organic and inorganic pollutant is presented in **Paper VI**. The recovery mechanism works
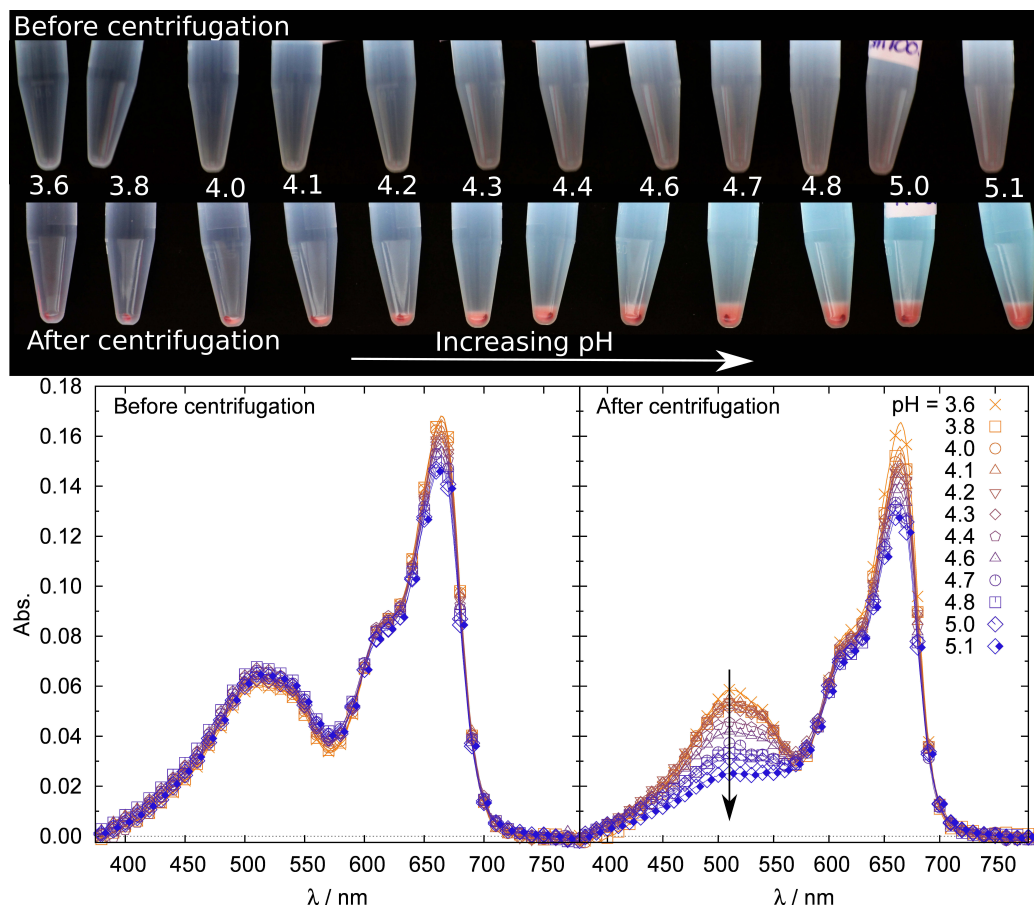
Figure 6.2 On the top, photos of chitosan - $C_{18:1}E_9Ac$ solutions containing Sudan Red (10 μM) and methylene blue (10 μM) with $Z = [-]/[+] = 0.2$, chitosan concentration of ~ 0.3 wt% and variable pH, before and after centrifugation are reported. On the bottom, the corresponding UV-Vis spectra are given.

as follows: i) the target compound is bound to the surfactant micelle or solubilized within its hydrophobic core; ii) given the pH is sufficiently high, the micelles are incorporated in the supramolecular complex and iii) can be centrifuged out of solution. This mechanism becomes clearly visible, when chitosan $- C_{18:1}E_9Ac$ complexes are employed for the separation of a mixture of an hydrophobic (Sudan red) and hydrophilic (methylene blue) dye. After centrifugation, an initially purple solution is separated into a red precipitate and a blue supernatant, as shown in Figure 6.2. This process can be applied also to metal ions bound to the surfactant headgroup or involved in an hydrophobic complex with an appropriate ligand, as demonstrated in detail in **Paper VI**. The whole process is highly selective, with respect both to the

32
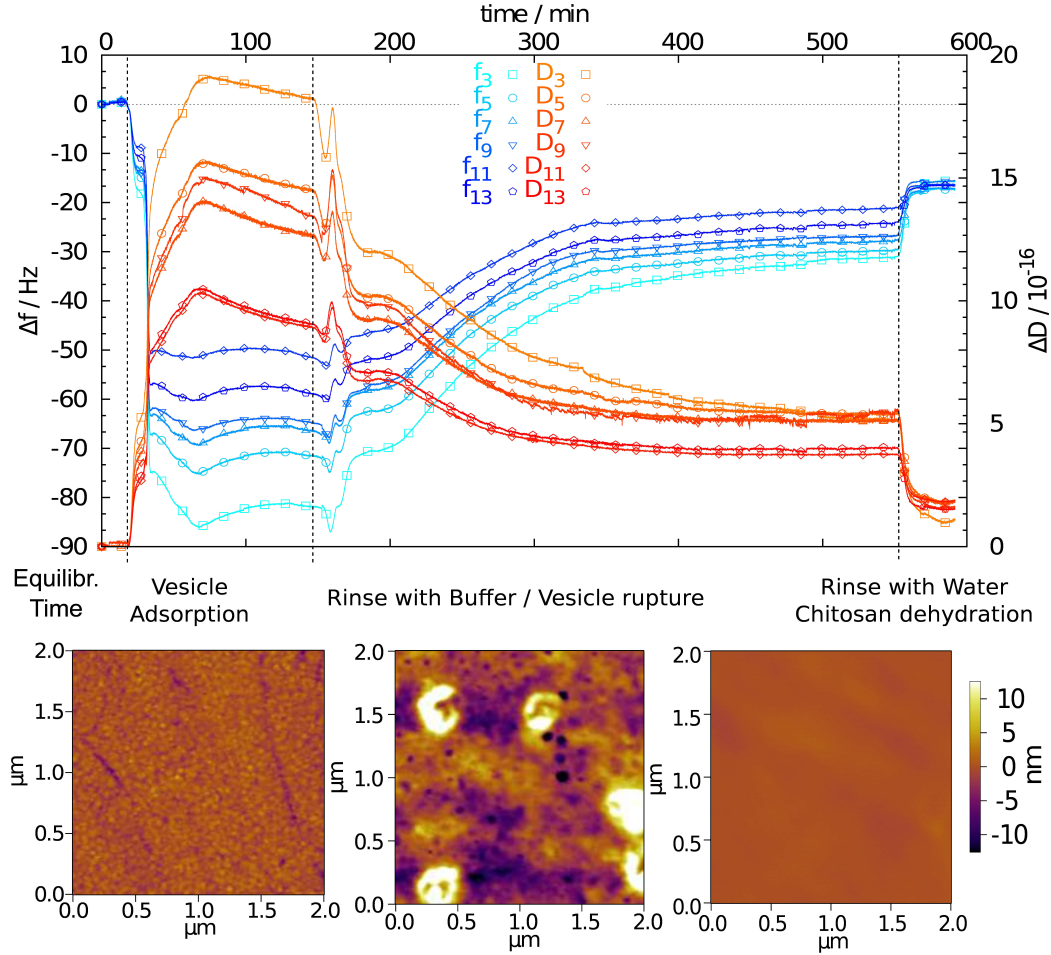
Figure 6.3 Top, frequency shift Δf and dissipation changes ΔD for different overtones during layer formation from chitosan – $C_{12}E_{4.5}Ac$, with chitosan concentration of 0.3 wt% and $Z = [-]/[+] = 0.4$ is reported. Bottom, AFM images of the QCM-D crystal before adsorption (0 min), after equilibration with the complex solution (~ 100 min), and after water rinse (~ 600 min). QCM-D measurements were performed on a E1 instrument from Q-Sense, at 25.00(2) °C and with a flow rate of 0.1 mL min^{-1}. For the experiments a Q-Sense QSX303 crystal was used. The fit with the Voigt-model was performed with the Q-Tools suite provided by Q-Sense, using a film density of 1.2 g cm^{-3}, and a solvent density and viscosity of 0.997 g cm^{-3} and 0.9 mPa s, respectively. AFM scans were performed on a Cypher AFM (Asylum Research) in air and tapping mode by Jana Lutzki.

33

hydrophilicity of the pollutant (in the case of organic molecules) as well as to the metal type and valence (in the case of heavy metals). For the latter case, the affinity can be tuned by the addition of an appropriate ligand.

The multiwalled vesicles, found in chitosan – $C_{12}E_{4.5}Ac$ mixtures, can be envisioned as carrier for hydrophilic molecules with release times which depend on the wall thickness, i.e., on the mixing ratio. However, another interesting approach is their use as precursors for "layer-by-layer" functionalization of surfaces. The simple idea consists of adsorbing the multilayered vesicles on a surface with their subsequent rupture and coverage of the surface. The adsorption process can be followed by quartz crystal microbalance with dissipation monitoring (QCM-D) and the morphology of the surface at different stages by atomic force microscopy (AFM). A preliminary experiment is shown in Fig. 6.3 and serves as a proof of principle.

The used protocol foresees an initial period in which the layer is in contact with the multiwalled vesicle solution, followed by a rinsing period with the buffer solution in which the complexes were prepared, and, finally, a rinse with pure water. When the crystal is in contact with the chitosan–$C_{12}E_{4.5}Ac$ solution, one observes a strong decrease in frequency and increase in dissipation, coupled with a strong splitting of the overtones (see Fig. 6.3 top). Such a behaviour is commonly found during the adsorption of vesicles,[76] as they are large and soft (high Δf and ΔD signals) and inhomogeneous in the z-direction (splitting of the overtones). The AFM image taken at this stage clearly shows the presence of spherical particles with a radius of ca. 200 nm, in perfect agreement with the structural picture of the multiwalled vesicles obtained by SANS and given in **Paper V**.

The subsequent rinse with buffer solution causes an increase in frequency and decrease in dissipation, together with a reduced splitting of the signals, indicating a pronounced mass loss, which can be ascribed to the rupture of the vesicles and the formation of a homogeneous multilayer on the surface. A layer thickness of ~ 30 nm is obtained when the QCM-D signal is described with the Voigt model for viscoelastic films.[77] This value is in good agreement with an expected film made up of 5 chitosan – surfactant layers, each 6 nm thick (see Table 3 in **Paper V**). The final rinse with water, where chitosan is insoluble while the surfactant is highly charged, causes a a further mass loss. The signals of the frequency shift from the different overtones are perfectly superimposed, while a small albeit significant splitting is observed in the dissipation signal, with the higher overtones showing a smaller dissipation. This indicates the presence of an hydrophobic outermost layer, given by the neutral chitosan chains. AFM images confirm the presence of a highly homogeneous layer on the crystal surface. The analysis of the QCM-D with both the Sauerbrey and Voigt model indicates the presence of a 3 nm thick layer,

suggesting the removal of the multilayer. Future work is planned foreseeing the optimization of the adsoprtion protocol as well as the confirmation of the presence of a multilayered structure by X-ray (or neutron) reflectometry.

Life is the art of drawing sufficient conclusions from insufficient premises.

Samuel Butler

7

Conclusions

Related to: Adv. Colloid Interf. Sci., **2015**, 220, 92–107.

Finally, after having introduced the general behaviour of ionic polysaccharide – surfactant mixtures and investigated in detail the mixtures of chitosan and alkyl oligoethyleneoxide carboxylic acids, a general overview of the behaviour of chitosan and small amphiphiles systems is given in **Paper VII**.

To summarize, oversimplifying certain aspects, it can be stated that for mixtures of ionic polysaccharides (and in particular of chitosan) and oppositely charged amphiphiles, the polymer only provides a stiff supramolecular skeleton for the aggregation of self-assembled amphiphilic molecules. The structure of the surfactant aggregate is solely determined by the ratio of headgroup size and hydrophobic volume, i.e., the surfactant packing parameter within the complex.

The structural characterization of chitosan and alkyl oligoethyleneoxide carboxylic acids reported in **Paper IV** and **Paper V** has shown that globular micelles are incorporated into the complex, with a supramolecular order depending on the strength of the interaction. Similarly, the bilayer structure of $C_{12}E_{4.5}Ac$ is retained within the complex, where multiwalled vesicles are formed. A seemingly contradicting result is given, for instance, by mixtures of the cationically modified cellulose JR-400 and sodium dodecyl
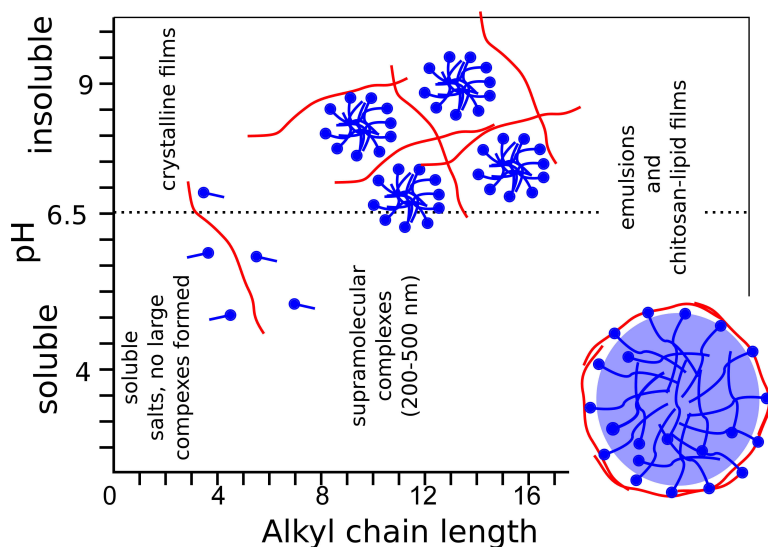
Figure 7.1 Schematic phase behaviour and structures of chitosan – carboxylic acid mixtures, depending on the solution pH and hydrophobicity of the organic acid.

sulfate,[26,78] where a sphere-to-rod transition for the surfactant aggregate is observed upon complexation. This transition can be explained by an apparent high ionic strength felt by the surfactant within the complex, i.e., with most of its charges being continuously compensated by those of the polymer, and therefore, by a reduced headgroup requirement which leads to the observed sphere-to-rod transition (as also found in pure alkyl sulfates or alkyl trimetylammonium solutions).[79,80]

The importance of the hydrophobic interactions can be evidenced in mixtures of chitosan and aliphatic carboxylic acid, whose phase behaviour is schematically reported in Fig. 7.1. The longer the alkyl chain of the carboxylic acid the stronger the hydrophobic interactions are. For instance, no aggregation is observed with short chain carboxylic acids $(n(C) \leq 5)$[81] as the necessary cooperative hydrophobic interaction is missing; mesostructured complexes are obtained with fatty acids with intermediate chain length $C_{11:1}$;[82–84] and, chitosan stabilized emulsions are formed for highly hydrophobic fatty acids $(n(C) > 16)$.[85,86]

Similar results as those reported for chitosan/$C_{12}E_{4.5}Ac$ mixtures are also found in systems where chitosan is mixed with phospholipid vesicles. Its addition promotes the formation of multilamellar vesicles and increases the membrane stiffness.[87,88] Moreover, the membranes become more resistant against pH, salt or temperature jumps.[89,90]

Polysaccharides are a great tool which nature wisely employed for the

fulfilment of highly different tasks. Their behaviour is therefore obviously complex. In this work, the focus was put on cellulose-based polysaccharides and chitosan. Both classes of polymers show an almost identical arrangement of functional groups (with the exception of an amine substituting an hydroxylic unit for cellulose/chitosan) and some common, peculiar characteristics were evidenced. For instance, the spacing between the charges and the intrinsic persistence length, elegantly agree with the Bjerrum length at physiological conditions. The first consequence is a strong tendency of these polymers to imprint a one-dimensional order to the resulting supramolecular aggregates (provided the curvature of the macroion is high enough to avoid an efficient adsorption). A second consequence arising from the chemical structure of the polymer is the complex interplay of interactions with other colloids. While the behaviour of many synthetic polyelectrolytes in mixtures with oppositely charged surfactant aggregates (or nm to μm sized objects in a more extended view) can be explained considering few effects, e.g., entropic effects arising from counterion release or polymer conformation loss, hydrophobic and dispersion interactions, the behaviour of polysaccharides is more complex. In addition to the just mentioned effects, specific interactions arising from the particular arrangements of functional groups do play a role.

Concluding, in the perspective of a sustainable economy, the use of biopolymers and bioderived polymers as an alternative to petro-based compounds is an unavoidable step, which, however, has to be coupled with a rational use of new materials and an efficient recycling process. In this regard, an added value of chitosan is its derivation from a waste product, crustaceans shells, which may limit in the future use on very large scales. However, the availability of chitin is nowadays orders of magnitude higher than its request. Differently, the availability of cellulose is virtually endless.

Finally, despite the highly complex behaviour of ionic polysaccharide – surfactant mixtures is far from being understood completely, reasonable explanations for a number of observations can be made, but accurate predictions are not (yet) possible. For example, some open questions directly linked to this work are: why do chitosan – sulfated surfactant complexes show such a low solubility? Why do polysaccharides with similar length collapse upon addition of surfactants while others gel? Why do chitosan – carboxylated surfactant mixtures seem to easily reach thermodynamic equilibrium while chitosan – sulfated surfactant do not? These, and many more questions are still open making polysaccharide – surfactant mixtures an interesting topic for further fundamental and applied research.

*The dwarf sees farther than the giant, when he has
the giant's shoulder to mount on.*

Samuel Taylor Coleridge

Bibliography

[1] Yarsley, V. E.; Couzens, E. G. *Plastics*; Allen Lane, Penguin Books, 1941; p 149.

[2] Staudinger, H. Über Polymerisation. *Berichte der Dtsch. Chem. Gesellschaft* **1920**, *53*, 1073–1085.

[3] Nobelprize.org, The Nobel Prize in Chemistry 1953. 1953; http://www.nobelprize.org/nobel_prizes/chemistry/laureates/1953/.

[4] Hopewell, J.; Dvorak, R.; Kosior, E. Plastics recycling: challenges and opportunities. *Philos. Trans. R. Soc. Lond. B. Biol. Sci.* **2009**, *364*, 2115–26.

[5] Vert, M.; Doi, Y.; Hellwich, K.-H.; Hess, M.; Hodge, P.; Kubisa, P.; Rinaudo, M.; Schué, F. Terminology for biorelated polymers and applications (IUPAC Recommendations 2012). *Pure Appl. Chem.* **2012**, *84*, 377–410.

[6] Corma, A.; Iborra, S.; Velty, A. Chemical routes for the transformation of biomass into chemicals. *Chem. Rev.* **2007**, *107*, 2411–502.

[7] Wasewar, K. L.; Yawalkar, A. a.; Moulijn, J. a.; Pangarkar, V. G. Fermentation of Glucose to Lactic Acid Coupled with Reactive Extraction: A Review. *Ind. Eng. Chem. Res.* **2004**, *43*, 5969–5982.

[8] Sarkar, N.; Ghosh, S. K.; Bannerjee, S.; Aikat, K. Bioethanol production from agricultural wastes: An overview. *Renew. Energy* **2012**, *37*, 19–27.

[9] Eriksson, K.-E.; Ljungdahl, L. G. In *Adv. Microb. Ecol.*; Marshall, K. C., Ed.; Advances in Microbial Ecology; Springer US: Boston, MA, 1985; Vol. 8; pp 237–299.

[10] Payen, A. Mémoire sur la composition du tissu propre des plantes et du ligneux. *Comptes Rendus* **1838**, *7*, 1052–1056.

[11] Karrer, P.; Hofmann, A. Polysaccharide XXXIX. Über den enzymatischen Abbau von Chitin und Chitosan I. *Helv. Chim. Acta* **1929**, *12*, 616–637.

[12] Medronho, B.; Romano, A.; Miguel, M. G.; Stigsson, L.; Lindman, B. Rationalizing cellulose (in)solubility: reviewing basic physicochemical aspects and role of hydrophobic interactions. *Cellulose* **2012**, *19*, 581–587.

[13] Rinaudo, M. Chitin and chitosan: Properties and applications. *Prog. Polym. Sci.* **2006**, *31*, 603–632.

[14] Klemm, D.; Heublein, B.; Fink, H.-P.; Bohn, A. Cellulose: fascinating biopolymer and sustainable raw material. *Angew. Chem. Int. Ed. Engl.* **2005**, *44*, 3358–93.

[15] Mourya, V.; Inamdar, N. Chitosan-modifications and applications: Opportunities galore. *React. Funct. Polym.* **2008**, *68*, 1013–1051.

[16] Roy, D.; Semsarilar, M.; Guthrie, J. T.; Perrier, S. Cellulose modification by polymer grafting: a review. *Chem. Soc. Rev.* **2009**, *38*, 2046–64.

[17] Feng, L.; Chen, Z.-l. Research progress on dissolution and functional modification of cellulose in ionic liquids. *J. Mol. Liq.* **2008**, *142*, 1–5.

[18] Kwak, J. C. T., Ed. *Polymer-Surfactant Systems*; Marcel Dekker, New York, 1998; p 482.

[19] Holmberg, K.; Jönsson, B.; Kronberg, B.; Lindman, B. *Surfactants and Polymers in Aqueous Solution*; John Wiley & Sons, Ltd: Chichester, UK, 2002; Vol. 2002; p 562.

[20] Antonietti, M.; Burger, C.; Effing, J. Mesomorphous polyelectrolyte-surfactant complexes. *Adv. Mater.* **1995**, *7*, 751–753.

[21] Antonietti, M.; Conrad, J.; Thuenemann, A. Polyelectrolyte-Surfactant Complexes: A New Type of Solid, Mesomorphous Material. *Macromolecules* **1994**, *27*, 6007–6011.

[22] Ober, C. K.; Wegner, G. Polyelectrolyte-Surfactant Complexes in the Solid State: Facile building blocks for self-organizing materials. *Adv. Mater.* **1997**, *9*, 17–31.

[23] Faul, C. F. J.; Antonietti, M. Facile synthesis of optically functional, highly organized nanostructures: dye-surfactant complexes. *Chem. - A Eur. J.* **2002**, *8*, 2764–8.

[24] Kästner, U.; Hoffmann, H.; Donges, R.; Ehrler, R.; Dönges, R. Interactions between modified hydroxyethyl cellulose (HEC) and surfactants. *Colloids Surf., A* **1996**, *112*, 209–225.

[25] Leung, P. S.; Goddard, E. D. Gels from dilute polymer/surfactant solutions. *Langmuir* **1991**, *7*, 608–609.

[26] Hoffmann, I.; Heunemann, P.; Prévost, S.; Schweins, R.; Wagner, N. J.; Gradzielski, M. Self-aggregation of mixtures of oppositely charged polyelectrolytes and surfactants studied by rheology, dynamic light scattering and small-angle neutron scattering. *Langmuir* **2011**, *27*, 4386–96.

[27] Tsianou, M.; Alexandridis, P. Control of the rheological properties in solutions of a polyelectrolyte and an oppositely charged surfactant by the addition of cyclodextrins. *Langmuir* **1999**, *15*, 8105–8112.

[28] Goddard, E. D. Polymer/surfactant interaction—Its relevance to detergent systems. *J. Am. Oil Chem. Soc.* **1994**, *71*, 1–16.

[29] Li, D.; Wagner, N. J. Universal binding behavior for ionic alkyl surfactants with oppositely charged polyelectrolytes. *J. Am. Chem. Soc.* **2013**, *135*, 17547–55.

[30] Piculell, L.; Lindman, B. Association and segregation in aqueous polymer/polymer, polymer/surfactant, and surfactant/surfactant mixtures: similarities and differences. *Adv. Colloid Interface Sci.* **1992**, *41*, 149–178.

[31] Ilekti, P.; Piculell, L.; Tournilhac, F.; Cabane, B. How To Concentrate an Aqueous Polyelectrolyte/Surfactant Mixture by Adding Water. *J. Phys. Chem. B* **1998**, *102*, 344–351.

[32] Tinland, B.; Pluen, A.; Sturm, J.; Weill, G.; Sadron-cnrs universite, I. C. Persistence Length of Single-Stranded DNA. *Macromolecules* **1997**, *30*, 5763–5765.

[33] Dobrynin, A. V. Electrostatic Persistence Length of Semiflexible and Flexible Polyelectrolytes. *Macromolecules* **2005**, *38*, 9304–9314.

[34] Ramachandran, R.; Beaucage, G.; Kulkarni, A. S.; McFaddin, D.; Merrick-Mack, J.; Galiatsatos, V. Persistence Length of Short-Chain Branched Polyethylene. *Macromolecules* **2008**, *41*, 9802–9806.

[35] Hoogendam, C. W.; de Keizer, A.; Cohen Stuart, M. A.; Bijster-bosch, B. H.; Smit, J. A. M.; van Dijk, J. A. P. P.; van der Horst, P. M.; Batelaan, J. G. Persistence Length of Carboxymethyl Cellulose As Evaluated from Size Exclusion Chromatography and Potentiometric Titrations. *Macromolecules* **1998**, *31*, 6297–6309.

[36] Buhler, E.; Boué, F. Chain Persistence Length and Structure in Hyaluronan Solutions: Ionic Strength Dependence for a Model Semirigid Polyelectrolyte. *Macromolecules* **2004**, *37*, 1600–1610.

[37] Lamarque, G.; Lucas, J.-m.; Viton, C.; Domard, A. Physicochemical Behavior of Homogeneous Series of Acetylated Chitosans in Aqueous Solution: Role of Various Structural Parameters. *Biomacromolecules* **2005**, *6*, 131–142.

[38] Ben-Naim, A. *Cooperativity and Regulation in Biochemical Processes*; Springer US: Boston, MA, 2001; pp 25–29.

[39] Freundlich, H. Über die adsorption in lösungen. *Zeitschrift für Phys.* **1906**, *57*, 385–470.

[40] Langmuir, I. THE CONSTITUTION AND FUNDAMENTAL PROPERTIES OF SOLIDS AND LIQUIDS. PART I. SOLIDS. *J. Am. Chem. Soc.* **1916**, *38*, 2221–2295.

[41] Langmuir, I. THE ADSORPTION OF GASES ON PLANE SURFACES OF GLASS, MICA AND PLATINUM. *J. Am. Chem. Soc.* **1918**, *40*, 1361–1403.

[42] Satake, I.; Yang, J. T. Interaction of sodium decyl sulfate with poly(L-ornithine) and poly(L-lysine) in aqueous solution. *Biopolymers* **1976**, *15*, 2263–75.

[43] Schwarz, G. Cooperative Binding to Linear Biopolymers. 1. Fundamental Static and Dynamic Properties. *Eur. J. Biochem.* **1970**, *12*, 442–453.

[44] Prévost, S.; Gradzielski, M. SANS investigation of the microstructures in catanionic mixtures of SDS/DTAC and the effect of various added salts. *J. Colloid Interface Sci.* **2009**, *337*, 472–84.

[45] Smith, L.; Hammond, R.; Roberts, K.; Machin, D.; McLeod, G. Determination of the crystal structure of anhydrous sodium dodecyl sulphate using a combination of synchrotron radiation powder diffraction and molecular modelling techniques. *J. Mol. Struct.* **2000**, *554*, 173–182.

[46] Paula, S.; Sues, W.; Tuchtenhagen, J. J.; Blume, A.; Siis, W.; Tuchtenhagen, J. J.; Blume, A. Thermodynamics of Micelle Formation as a Function of Temperature: A High Sensitivity Titration Calorimetry Study. *J. Phyical Chem.* **1995**, *99*, 11742–11751.

[47] Morfin, I.; Buhler, E.; Cousin, F.; Grillo, I.; Boué, F. Rodlike complexes of a polyelectrolyte (hyaluronan) and a protein (lysozyme) observed by SANS. *Biomacromolecules* **2011**, *12*, 859–70.

[48] Chiappisi, L.; Prévost, S.; Grillo, I.; Gradzielski, M. Chitosan/Alkylethoxy Carboxylates: A Surprising Variety of Structures. *Langmuir* **2014**, *30*, 1778–1787.

[49] Chiappisi, L.; Prévost, S.; Grillo, I.; Gradzielski, M. From crab shells to smart systems: chitosan-alkylethoxy carboxylate complexes. *Langmuir* **2014**, *30*, 10608–16.

[50] Shi, L.; Carn, F.; Boué, F.; Mosser, G.; Buhler, E. Nanorods of Well-Defined Length and Monodisperse Cross-Section Obtained from Electrostatic Complexation of Nanoparticles with a Semiflexible Biopolymer. *ACS Macro Lett.* **2012**, *1*, 857–861.

[51] Shi, L.; Carn, F.; Boué, F.; Mosser, G.; Buhler, E. Control over the electrostatic self-assembly of nanoparticle semiflexible biopolyelectrolyte complexes. *Soft Matter* **2013**, *9*, 5004–15.

[52] Chiappisi, L.; Prévost, S.; Gradzielski, M. Form factor of cylindrical superstructures composed of globular particles. *J. Appl. Crystallogr.* **2014**, *47*, 827–834.

[53] Debye, P. Zerstreuung von Röntgenstrahlen. *Ann. Phys.* **1915**, *351*, 809–823.

[54] Tarafdar, A.; Biswas, G. Extraction of Chitosan from Prawn Shell Wastes and Examination of its Viable Commercial Applications. *Int. J. Theor. Appl. Res. Mech. Eng.* **2013**, *2*, 17–24.

[55] Pochanavanich, P.; Suntornsuk, W. Fungal chitosan production and its characterization. *Lett. Appl. Microbiol.* **2002**, *35*, 17–21.

[56] Chatterjee, S.; Adhya, M.; Guha, A.; Chatterjee, B. Chitosan from Mucor rouxii: production and physico-chemical characterization. *Process Biochem.* **2005**, *40*, 395–400.

[57] Chen, M.-C.; Mi, F.-L.; Liao, Z.-X.; Hsiao, C.-W.; Sonaje, K.; Chung, M.-F.; Hsu, L.-W.; Sung, H.-W. Recent advances in chitosan-based nanoparticles for oral delivery of macromolecules. *Adv. Drug Deliv. Rev.* **2013**, *65*, 865–79.

[58] Dutta, P.; Dutta, J.; Tripathi, V. Chitin and chitosan: Chemistry, properties and applications. *J. Sci. Ind. Res. (India).* **2004**, *63*, 20–31.

[59] Babak, V.; Merkovich, E. A.; Desbrières, J.; Rinaudo, M. Formation of an ordered nanostructure in surfactant-polyelectrolyte complexes formed by interfacial diffusion. *Polym. Bull.* **2000**, *45*, 77–81.

[60] Thongngam, M.; McClements, D. J. Influence of pH, ionic strength, and temperature on self-association and interactions of sodium dodecyl sulfate in the absence and presence of chitosan. *Langmuir* **2005**, *21*, 79–86.

[61] Onésippe, C.; Lagerge, S. Studies of the association of chitosan and alkylated chitosan with oppositely charged sodium dodecyl sulfate. *Colloids Surf., A* **2008**, *330*, 201–206.

[62] Lundin, M.; Macakova, L.; Dedinaite, A.; Claesson, P. M. Interactions between chitosan and SDS at a low-charged silica substrate compared to interactions in the bulk–the effect of ionic strength. *Langmuir* **2008**, *24*, 3814–27.

[63] Rinaudo, M.; Kil'deeva, N. R.; Babak, V. Surfactant-polyelectrolyte complexes on the basis of chitin. *Russ. J. Gen. Chem.* **2008**, *78*, 2239–2246.

[64] Thongngam, M.; McClements, D. J. Characterization of Interactions between Chitosan and an Anionic Surfactant. *J. Agric. Food. Chem.* **2004**, *52*, 987–991.

[65] Onésippe, C.; Lagerge, S. Study of the complex formation between sodium dodecyl sulfate and chitosan. *Colloids Surf., A* **2008**, *317*, 100–108.

[66] Wei, Y. C.; Hudson, S. M. Binding of sodium dodecyl sulfate to a polyelectrolyte based on chitosan. *Macromolecules* **1993**, *26*, 4151–4154.

[67] Renoncourt, A.; Bauduin, P.; Nicholl, E.; Touraud, D.; Verbavatz, J.-M.; Dubois, M.; Drechsler, M.; Kunz, W. Spontaneous vesicle formation of an industrial single-chain surfactant at acidic pH and at room-temperature. *Chemphyschem* **2006**, *7*, 1892–6.

[68] Schwarze, M.; Chiappisi, L.; Prévost, S.; Gradzielski, M. Oleylethoxy-carboxylate - An efficient surfactant for copper extraction and surfactant recycling via micellar enhanced ultrafiltration. *J. Colloid Interface Sci.* **2014**, *421*, 184–90.

[69] McQuigg, D. W.; Kaplan, J. I.; Dubin, P. L. Critical conditions for the binding of polyelectrolytes to small oppositely charged micelles. *J. Phys. Chem.* **1992**, *96*, 1973–1978.

[70] Leonard, M. J.; Strey, H. H. Phase Diagrams of Stoichiometric Polyelectrolyte−Surfactant Complexes. *Macromolecules* **2003**, *36*, 9549–9558.

[71] Moss, J. M.; Van Damme, M. P.; Murphy, W. H.; Preston, B. N. Dependence of salt concentration on glycosaminoglycan-lysozyme interactions in cartilage. *Arch. Biochem. Biophys.* **1997**, *348*, 49–55.

[72] Seyrek, E.; Dubin, P. L.; Tribet, C.; Gamble, E. A. Ionic strength dependence of protein-polyelectrolyte interactions. *Biomacromolecules* **2003**, *4*, 273–82.

[73] Wang, X.; Li, Y.; Li, J.; Wang, J.; Wang, Y.; Guo, Z.; Yan, H. Salt effect on the complex formation between polyelectrolyte and oppositely charged surfactant in aqueous solution. *J. Phys. Chem. B* **2005**, *109*, 10807–12.

[74] Matsuda, T.; Annaka, M. Salt Effect on Complex Formation of Neutral / Polyelectrolyte Block Copolymers and Oppositely Charged Surfactants. *Science (80-.).* **2008**, *24*, 5707–5713.

[75] Pojják, K.; Bertalanits, E.; Mészáros, R.; Pojj, K. Effect of salt on the equilibrium and nonequilibrium features of polyelectrolyte/surfactant association. *Langmuir* **2011**, *27*, 9139–47.

[76] Richter, R. P.; Bérat, R.; Brisson, A. R. Formation of solid-supported lipid bilayers: an integrated view. *Langmuir* **2006**, *22*, 3497–505.

[77] Voinova, M. V.; Rodahl, M.; Jonson, M.; Kasemo, B. Viscoelastic Acoustic Response of Layered Polymer Films at Fluid-Solid Interfaces: Continuum Mechanics Approach. *Phys. Scr.* **1999**, *59*, 391–396.

[78] Hoffmann, I.; Farago, B.; Schweins, R.; Falus, P.; Sharp, M.; Gradzielski, M. Structure and dynamics of polyelectrolytes in viscous polyelectrolyte-surfactant complexes at the mesoscale. *EPL (Europhysics Lett.* **2013**, *104*, 28001.

[79] Gamboa, C.; Rios, H.; Sepulveda, L. Effect of the nature of counterions on the sphere-to-rod transition in cetyltrimethylammonium micelles. *J. Phys. Chem.* **1989**, *93*, 5540–5543.

[80] Missel, P. J.; Mazer, N. A.; Benedek, G. B.; Carey, M. C. Influence of chain length on the sphere-to-rod transition in alkyl sulfate micelles. *J. Phys. Chem.* **1983**, *87*, 1264–1277.

[81] Demarger-André, S.; Domard, A. Chitosan carboxylic acid salts in solution and in the solid state. *Carbohydr. Polym.* **1994**, *23*, 211–219.

[82] Demarger-André, S.; Domard, A. Chitosan behaviours in a dispersion of undecylenic acid. *Carbohydr. Polym.* **1993**, *22*, 117–126.

[83] Demarger-André, S.; Domard, A. Chitosan behaviours in a dispersion of undecylenic acid. morphological aspects. *Carbohydr. Polym.* **1995**, *27*, 101–107.

[84] Demarger-André, S.; Domard, A. Chitosan behaviours in a dispersion of undecylenic acid. Structural parameters. *Carbohydr. Polym.* **1994**, *24*, 177–184.

[85] Reis, A. B.; Yoshida, C. M.; Franco, T. T.; Reis, A. P. C. Application of chitosan emulsion as a coating on Kraft paper. *Polym. Int.* **2011**, *60*, 963–969.

[86] Dimzon, I. K. D.; Ebert, J.; Knepper, T. P. The interaction of chitosan and olive oil: effects of degree of deacetylation and degree of polymerization. *Carbohydr. Polym.* **2013**, *92*, 564–70.

[87] Mertins, O.; Dimova, R. Insights on the interactions of chitosan with phospholipid vesicles. Part II: Membrane stiffening and pore formation. *Langmuir* **2013**, *29*, 14552–9.

[88] Gerelli, Y.; Di Bari, M. T.; Barbieri, S.; Sonvico, F.; Colombo, P.; Natali, F.; Deriu, A. Flexibility and drug release features of lipid/saccharide nanoparticles. *Soft Matter* **2010**, *6*, 685.

[89] Mertins, O.; Lionzo, M. I.; Micheletto, Y. M.; Pohlmann, A. R.; da Silveira, N. P. Chitosan effect on the mesophase behavior of phosphatidylcholine supramolecular systems. *Mater. Sci. Eng. C* **2009**, *29*, 463–469.

[90] Quemeneur, F.; Rammal, A.; Rinaudo, M.; Pépin-Donat, B. Large and giant vesicles "decorated" with chitosan: effects of pH, salt or glucose stress, and surface adhesion. *Biomacromolecules* **2007**, *8*, 2512–9.

In addition to the here reported bibliography refer also to the articles cited in the manuscript papers.

A
Appendix

A.1 Satake-Yang ITC fit

```python
import scipy
import scipy.optimize, scipy.special, scipy.stats
from math import sqrt
import matplotlib
import matplotlib.pyplot as plt
from numpy import loadtxt
from numpy import savetxt
from pylab import *
from scipy.optimize import fsolve
from scipy.optimize import curve_fit


#K is the non-cooperative binding constant
#Ku is the cooperative binding constant
#DHNC is the non-cooperative binding enthalpy
#DHC is the cooperative binding enthalpy
#CP is total binding site concentration
#Ctot is the total surfactant concentration
#Cf is the free surfactant concentration

#This function is obtained by combining the adsoprtion isotherm with
#the mass balance equation. It is used by Sig() to determine Theta
#as a function of the total surfactant concentration.
def func(x, Ctot, CP, K, u):
    S = x-0.5*(1+(K*u*(Ctot-CP*x)-1)/
```

```python
            sqrt((1−K*u*(Ctot−CP*x))**2+4*K*(Ctot−CP*x)))
    return S


def Sig(Ctot, Ku, u, DHNC, DHC):
    CP = 2.
    K = Ku/u
#Determines the free surfactant concentration from the binding isotherm
#and mass balance
    Theta = fsolve(func, Ctot/1.5, args=(Ctot, CP, K, u))
#Calculates CF from the mass balance
    Cf = Ctot−CP*Theta
#lambda0, eigenvalue from weight matrix
    lamb = 1. + sqrt((K*Cf*Theta)/(1.−Theta))
#fraction of non−cooperatively bound surfactant
    chi = (Cf*(1.−Theta)*K)/(Theta*lamb**2)
#new variable
    s = K*u*Cf
#first derivative of theta with respect to cf
    Theta1cf = 0.5*((u*K)/sqrt((s−1)**2+4*s/u)−
        ((s−1)*(2*u*K*(s−1)+4*K))/(2*sqrt((s−1)**2+4*s/u)**3))
#set of dummy functions to calculate chi1cf
    a1 = −(4.0*Cf*Theta1cf*K)/(Theta*(sqrt((1−s)**2+4*s/u)+s+1)**2)
    a2 = −(4.0*Cf*(1−Theta)*Theta1cf*K)/
        (Theta**2*(sqrt((1−s)**2+4*s/u)+s+1)**2)
    a3 = +(4.0*(1−Theta)*K)/(Theta*(sqrt((1−s)**2+4*s/u)+s+1)**2)
    a4 = −(8.0*Cf*(1−Theta)*K*((4*K−2*u*K*(1−s))/
        (2*sqrt((1−s)**2+4*s/u))+u*K))/
            (Theta*(sqrt((1−s)**2+4*s/u)+s+1)**3)
#first derivative of chi with respect to Cf
    chi1cf = a1 + a2 + a3 + a4
#mean enthalpy of adsorption
    DHm=DHNC*chi+(1−chi)*DHC
#calorimetric signal
    return CP*(Theta1cf*DHm + Theta*(DHNC−DHC)*chi1cf)/
            (CP*Theta1cf+1)


#Reads from the file the total surfactant concentration
#and the binding heat
Ctot, Y = loadtxt('input.dat', unpack=True)

#Initial guess of the fitting parameters
#in the order as the appear in Sig()
guess = [2., 510., 1000., 2000.]
params = guess
#Fit command. Calculates the set of best fitting parameters
#and their covariance matrix. Standard deviation is obtained
#as the square root of the values on the diagonal.
params, params_covariance = curve_fit(Sig, Ctot, Y, guess)
```

```python
#print params #Prints in  terminal the parameter matrix
#print params_covariance #Prints in terminal the covariance matrix

Ctotcalc = arange(0.002,2,0.002)
# In the following lines the experimental data and
#best fitting curve are plotted
matplotlib.rcParams['axes.unicode_minus'] = False
fig = plt.figure()
ax = fig.add_subplot(111)
ax.set_xscale('log')
ax.plot(Ctot,Sig(Ctot, params[0], params[1], params[2], params[3]))
ax.plot(Ctot, Y, 'o')
plt.show()
#End of the program

savetxt('Sig.out', Sig(Ctot, params[0], params[1],
        params[2], params[3]))
savetxt('Ctot.out', Ctot)
```

A.2 Sasfit form factor for N-core-shell ellipsoids aligned within a cylinder

```
#include "include/private.h"
#include <sasfit_error_ff.h>

// define shortcuts for local parameters/variables
#define A       param->p[0]   //Rotational axis
#define B       param->p[1]   //Equatiorial axis
#define T       param->p[2]   //Shell thickness
#define D       param->p[3]   //Border-to-border distance
#define N       param->p[4]   //Number of micelles in the cylinder
#define RHO_P   param->p[5]   //SLD of the particle core
#define RHO_S   param->p[6]   //SLD of the particle shell
#define RHO_C   param->p[7]   //SLD of the cylinder


scalar sasfit_ff_chitosan_ellipsoids_f1(scalar x, sasfit_param * param)
{
        SASFIT_ASSERT_PTR(param); // assert pointer param is valid
        double prefacelel, prefaccylel;
        double Q = param->p[MAXPAR-1];
        double vcyl = param->p[MAXPAR-8];
        double R = param->p[MAXPAR-6];
        double L = param->p[MAXPAR-7];
        // End importing parameters
        double xc = Q*sqrt(gsl_pow_2(A*x) + gsl_pow_2(B)*(1.0-x*x));
        double xs = Q*sqrt(gsl_pow_2((A+T)*x) + gsl_pow_2(B+T)*(1.0-x*x));
        double vc = 4.0/3.0*M_PI*A*B*B;
        double vs = 4.0/3.0*M_PI*(A+T)*(B+T)*(B+T);
        double y = Q*(D+2.*(A+T))*x;
        double fc = vc*(RHO_P-RHO_S)*3.0*(sin(xc)-xc*cos(xc))/gsl_pow_3(xc);
        double fs = vs*(RHO_S-RHO_C)*3.0*(sin(xs)-xs*cos(xs))/gsl_pow_3(xs);
        double fcyl = vcyl*RHO_C*4.0*gsl_sf_bessel_J1(Q*R*sqrt(1.0-x*x))*
                sin(Q*L*x/2.0)/(Q*Q*R*sqrt(1.0-x*x)*L*x);

        prefacelel = (1.-cos(y*N))/(1.-cos(y));
        prefaccylel = cos(y*N/2.)*sin(y*(N+1)/2.)/sin(y/2.)-1.;

        double Aelel = gsl_pow_2(fc+fs)*prefacelel;
        double Acylcyl = gsl_pow_2(fcyl);
        double Acylel = fcyl*(fc+fs)*prefaccylel;
        return Aelel + Acylcyl + 2.*Acylel;


}
```

```
scalar sasfit_ff_cs_ellipsoid_in_cyl(scalar q, sasfit_param * param)
{
        SASFIT_ASSERT_PTR(param); // assert pointer param is valid

        SASFIT_CHECK_COND1((q < 0.0), param, "q(%lg) < 0",q);
        SASFIT_CHECK_COND1((A < 0.0), param, "A(%lg) < 0",A);
        SASFIT_CHECK_COND1((B < 0.0), param, "B(%lg) < 0",B);
        SASFIT_CHECK_COND1((T < 0.0), param, "T(%lg) < 0",T);
        SASFIT_CHECK_COND1((D < 0.0), param, "D(%lg) < 0",D);
        SASFIT_CHECK_COND1((N < 0.0), param, "N(%lg) < 0",N);

        double R = B + T; // Radius of the cylinder
        double L = N*(2*(A+T) + D); // Length of the cylinder
        double Vcyl = M_PI*R*R*L; // Volume of the cylinder

        param->p[MAXPAR-1] = q;
        param->p[MAXPAR-6] = R;
        param->p[MAXPAR-7] = L;
        param->p[MAXPAR-8] = Vcyl;
        scalar res;

        res = sasfit_integrate(0.0,1.0,sasfit_ff_chitosan_ellipsoids_f1,param);
                                //radial average of object with N particles
        return res;
}
```

List of symbols and abbreviations

δ Debye length

ΔD Dissipation change

Δf Frequency shift

ΔH^c Cooperative binding heat

ΔH^{nc} Non-cooperative binding heat

λ Wavelength

λ_B Bierrum length

Ku   Cooperative binding constant

K   Non-cooperative binding constant

n   Refractive index

Θ Binding isotherm

θ Scattering angle

ε_0 Vacuum permittivity

ε_r Relative permittivity

C_f Free surfactant concentration

e_0 Elementary charge

I Ionic strength

k_B Boltzmann constant

l_p Persistence length

l_p^e	Electrostatic contribution to the persistence length
l_p^i	Intrinsic persistence length
N_A	Avogadro constant
q	Modulus of the scattering vector
U_e	Electrostatic potential energy
Z	Mixing ratio
AFM	Atomic force microscopy
DLS	Dynamic light scattering
FCS	Fluorescence correlation spectroscopy
PE	Polyelectrolyte
QCM-D	Quartz crystal microbalace with dissipation monitoring
R	Gas constant
SANS	Small-angle neutron scattering
SAXS	Small-angle x-ray scattering
SLS	Static light scattering
SPEC	Surfactant – Polyelectrolyte complex
T	Absolute temperature

Full-text manuscripts are available online as follows:

- **Paper I** Complexes of oppositely charged polyelectrolytes and surfactants – recent developments in the field of biologically derived polyelectrolytes. L. Chiappisi, I. Hoffmann and M. Gradzielski. *Soft Matter*, **2013**, *9*, 3896-3909. Available at http://dx.doi.org/10.1039/c3sm27698h.

- **Paper II** An improved method for analyzing isothermal titration calorimetry data from oppositely charged surfactant polyelectrolyte mixtures. L.Chiappisi, D. Li, N. J. Wagner, M. Gradzielski. *The Journal of Chemical Thermodynamics*, **2014**, *68*, 48-52. Available at http://dx.doi.org/10.1016/j.jct.2013.08.027.

- **Paper III** Form factor of cylindrical superstructures composed of globular particles. L. Chiappisi, S. Prévost, M. Gradzielski. *Journal of Applied Crystallography*, **2014**, *47*, 827-834. Available at http://dx.doi.org/10.1107/S1600576714005524.

- **Paper IV** Chitosan/Alkylethoxy Carboxylates: A Surprising Variety of Structures. L. Chiappisi, S. Prévost, I. Grillo, M. Gradzielski. *Langmuir*, **2014**, *30*, 1778-1787. Available at http://dx.doi.org/10.1021/la404718e.

- **Paper V** From Crab Shells to Smart Systems: Chitosan–Alkylethoxy Carboxylate Complexes. L. Chiappisi, S. Prévost, I. Grillo, M. Gradzielski. *Langmuir*, **2014**, *30*, 10608-10616. Available at http://dx.doi.org/10.1021/la502569p.

- **Paper VI** Towards bioderived intelligent nanocarriers for controlled pollutant recovery and pH-sensitive binding. L. Chiappisi, M. Simon, M. Gradzielski. *ACS applied Materials & Interfaces*, **2015**, *7*, 6139-6145. Available at http://dx.doi.org/10.1021/am508846r.

- **Paper VII** Co-assembly in Chitosan – Surfactant mixtures: thermodynamics, structures and applications. L. Chiappisi, M. Gradzielski *Advances in Colloid and Interfaces*, **2015**, *220*, 92-107. doi: Available at http://dx.doi.org/10.1016/j.cis.2014.10.013.